

CONTROL - DISPLAY INTEGRATION PROGRAM

AD 652496

DEVELOPMENT OF HIGH CONTRAST ELECTROLUMINESCENT DISPLAYS

SIDNEY V. PETERTYL, DR. PAUL R. FULLER, CHESTER A. WYSOCKI,
et al.

INSTRUMENT DIVISION
LEAR SIEGLER, INC.

TECHNICAL REPORT AFFDL-TR-66-183

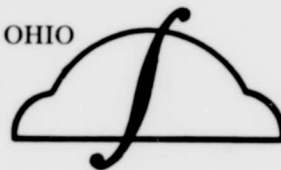
MARCH 1967

DDC
RECEIVED
JUN 5 1967
RECEIVED
D

Distribution of this document is unlimited.

AIR FORCE FLIGHT DYNAMICS LABORATORY
RESEARCH AND TECHNOLOGY DIVISION
AIR FORCE SYSTEMS COMMAND
WRIGHT-PATTERSON AIR FORCE BASE, OHIO

ARCHIVE COPY



AFFDL-TR-66-183

**DEVELOPMENT OF HIGH CONTRAST
ELECTROLUMINESCENT DISPLAYS**

*SIDNEY V. PETERTYL, DR. PAUL R. FULLER, CHESTER A. WYSOCKI,
et al.*

*INSTRUMENT DIVISION
LEAR SIEGLER, INC.*

Distribution of this document is unlimited.

FOREWORD

This program was initiated by the Control Systems Research Branch, Flight Control Division, of the Air Force Flight Dynamics Laboratory, under Task 619009, "Advanced Display Generation Techniques" through the direction and assistance of Major Loren A. Anderson, Mr. John H. Kearns, III, Mr. Edward L. Warren and Mr. Charles A. Shoals. Captain Carlton J. Peterson served as the Task Scientist and Contract Monitor of the high-contrast display program since its inception.

The studies presented began in June 1965, under Contract AF33(615)-2841 with the Solid-State Display Department of the Instrument Division of Lear Siegler, Inc. and were concluded in December 1966. The chief contributors were Sidney V. Petertyl, Dr. Paul R. Fuller, Chester A. Wysocki, Ivan E. Buck, and Robert J. Kurti.

The manuscript was released by the authors on February 1967 for publication as an RTD technical documentary report and bears the LSI report number GRR-67-1268.

This program has resulted in a significant contribution to the field of electro-optics and, as such, represents an important step in the development of a whole new family of legible aircraft, spacecraft, and ground-based display systems. It has been possible, in effect, to successfully take the technology of emission displays from the darkroom to the bright ambient conditions of the cockpit in one stride.

Recognition for this development rests solely with the originating Air Force Agency and the scientific community of Lear Siegler, Inc.

This report has been reviewed and is approved.



Loren A. Anderson, Major, USAF
Chief, Control Systems Research Branch
Flight Control Division

ABSTRACT

This report describes the development, characterization, and human factors evaluation of high visibility electroluminescent displays. Through the development of a greatly improved contrast filter technique and its combination with anti-reflection coatings, it is shown that daylight aircraft cockpit EL displays can be made. The importance of both specular and diffuse reflections are illustrated. A dramatic reduction in the display brightness required for the threshold of rapid readability has been achieved. Improving display visibility by use of high contrast rather than high brightness means that electrical power dissipation for the display can be reduced, and useful display life increased.

Distribution of this abstract is unlimited.

TABLE OF CONTENTS

Section		Page No.
I	INTRODUCTION	1
	1. Statement of The Problem	2
	2. Prior State of The Art	3
II	SUMMARY OF RESULTS	5
	1. General Principle of High Contrast EL Displays	5
	2. Program Accomplishments	6
III	TECHNIQUE DEVELOPMENT	10
	1. Optical Considerations	10
	a. Reflections and Their Sources	10
	b. Methods for Reducing Reflections	10
	2. Techniques and Measurements	26
	a. Measuring Techniques	26
	b. Contrast Filter Measurements	26
	c. Anti-Reflection Coating Measurements	43
IV	HUMAN FACTORS STUDY	50
	1. Methods and Results	50
	2. Conclusions	56
APPENDIX	EXTINCTION AND DISPERSION IN A MEDIUM CONTAINING PARTICLES	57
	REFERENCES	62
	BIBLIOGRAPHY	63

LIST OF ILLUSTRATIONS

Figure		Page No.
1.	Conventional and High-Contrast EL Under Identical Incident Illumination	4
2.	Experimental Altimeter Display Before Assembly	8
3.	Experimental Altimeter Display After Assembly	9
4.	Reflection Coefficients Vs. Ratio of Indices	16
5.	Scattering Efficiency Vs. Size Factor for Various Ratios of Indices	21
6.	Efficiency Factor for Absorption as a Function of X, the Particle Size Factor and the Absorption Coefficient, K. ($N = 1.5 - iK$)	22
7.	Efficiency Factor for Scattering as a Function of X, the Particle Size Factor and the Absorption Coefficient, K. ($N = 1.5 - iK$)	23
8.	White Diffuse Standard (98% Reflectance) Light Source Normal to Surface	27
9.	White Diffuse Standard (98% Reflectance) Light Source 45° From Normal to Surface	28
10.	Percent Reflectance of Conventional EL Lamp	29
11.	Percent Reflectance of Conventional EL Lamp	30
12.	Percent Reflectance From Surface of High-Contrast Layer With No Insulating Layer Behind the High-Contrast Layer	32
13.	Percent Reflectance From Surface of High-Contrast Layer With Insulating Layer Behind The High-Contrast Layer	33
14.	Percent Transmission Vs. Viewing Angle for EL Lamp With High-Contrast Layer	34
15.	Percent Reflectance of EL Lamp With High-Contrast Layer	36
16.	Percent Reflectance of EL Lamp With 20% - Transmitting High-Contrast Layer	37
17.	Percent Reflectance of EL Lamp With 30% - Transmitting High-Contrast Layer	38

LIST OF ILLUSTRATIONS (cont)

Figure		Page No.
18.	Percent Reflectance of EL Lamp With 40%- Transmitting High-Contrast Layer	39
19.	Percent Reflectance of EL Lamp With 50%- Transmitting High-Contrast Layer	40
20.	Luminance Vs. Voltage High Contrast Layer Position Variable	42
21.	Percent Reflectance of EL Lamp With 30%- Transmitting Gray Glass Substrate	44
22.	Percent Reflectance of High Contrast EL Lamp With HEA Coating on Front Surface	45
23.	Percent Reflectance of High Contrast EL Lamp With Trucite Coating on Front Surface	46
24.	Percent Reflectance of High-Contrast EL Lamp With Velvetone Coating on Front Surface	47
25.	Percent Reflectance of EL Landing Sequence Lamp	49
26.	Terradyne Part-Task Simulator	51
27.	Regular, High-Contrast, and Improved High- Contrast Displays	52

LIST OF SYMBOLS

a_n	Mie coefficient
b_n	Mie coefficient
CR	Contrast ratio
$h_m^2 ()$	Spherical Hänkel function of the second kind
I	Intensity of scattered light
I_0	Intensity of incident light
i_1	Square of amplitude function S_1
i_2	Square of amplitude function S_2
$j_n ()$	Spherical Bessel function
L	Luminance
N	Ratio of indices of refraction
Q_{ext}	Efficiency factor for extinction
Q_{sca}	Efficiency factor for scattering
Q_{obs}	Efficiency factor for absorption
R	Distance from particle
r	Radius of particle
Re	Real part of complex number
S_1	Complex amplitude function of wave polarized perpendicular to scattering plane
S_2	Complex amplitude function of wave polarized parallel to scattering plane
x	Particle size factor

α	Absorption coefficient
η	Real part of index of refraction
η'	Complex index of refraction
θ	Angle of incidence
θ_c	Critical angle for external incidence
K	Absorption index
λ	Wavelength
λ_m	Waveiength in medium
π_n	Associated legendre polynominal
ρ	Reflection factor
ρ_0	Reflection factor for normal incidence
$\rho_{ }$	Reflection factor for parallel polarized light
ρ_{\perp}	Reflection factor for perpendicularly polarized light
ρ_e	Reflection factor for externally incident light
ρ_i	Reflection factor for internally incident light
σ_{ext}	Extinction cross-section
σ_{sco}	Scattering cross-section
σ_{obs}	Absorption cross-section
σ_{bsco}	Backscattering cross-section
τ_n	Associated legendre polynomial
ϕ	Angle of refraction
ϕ_c	Critical angle for internal incidence
ω	Wave number

SECTION I

INTRODUCTION

The successful development of techniques to greatly improve the contrast and visibility of electroluminescent (EL) displays has been achieved.

The principle discoveries that led to this achievement were:

- Opaque particle filters are much more effective than optically clear, uniformly absorbing filters.
- Specular reflections from the air-glass and glass-front electrode interfaces must be minimized in order to realize the full benefit of the contrast filter.

The effectiveness of the techniques developed in this program were validated by the Air Force Flight Dynamics Laboratory through the use of high-contrast EL displays in a T-39 aircraft during numerous daylight flights. Comments and recommendations resulting from this flight test program were invaluable in determining the directions to be taken to perfect high-contrast techniques.

The high-contrast EL display technology produced during this program has been applied to two other Lear-Siegler efforts with the Flight Dynamics Laboratory.

Three different high contrast EL displays were used on Contract #AF 33(615)-2538, "Landing Indicators". Two of these utilized rate analog, moving EL fields, in conjunction with a null pointer, to display vertical velocity and horizontal displacement. The third instrument displayed landing event sequence information.

The other effort to use these high-contrast techniques was "Solid-State" Altimeter, Contract #AF33(615)-3871. This experimental display uses three colors of EL emission -- green, white, and amber. The following information is presented in this display:

- a. Radar altitude -- bar graph
- b. Vertical velocity - pointer
- c. Command altitude differential - pointer
- d. Barometric altitude - moving scale
- e. Barometric pressure - numeric
- f. Barometric altitude -- numeric
- g. Command altitude -- numeric
- h. Vertical velocity -- numeric

In addition, high-contrast EL display techniques are now being specified for flight hardware by NASA for the Apollo program and by the Air Force for the MOL. Both of these actions are, at least partly, a direct result of the work discussed in this report.

The principles of contrast enhancing that are discussed in this report should be considered for application to other display techniques, such as rear projection screens and cathode ray tubes.

1. STATEMENT OF THE PROBLEM

Objects or patterns are perceived visually because of differences in the color and/or intensity of reflected or emitted light. Therefore, detail is seen only because it contrasts in color or brightness with its immediate surroundings.

Considering the traditional black and white light absorbing and reflecting display, such as this printed page, the above statement about visual perception seems almost too simple and obvious to warrant mentioning. The contrast relationship in this most familiar case is often taken for granted because the contrast between the information and its background remains essentially constant through wide variations in the intensity of incident light. The contrast and visibility of such displays only diminish as the incident light intensity becomes low.

With EL and other light emitting displays the visibility situation is reversed. Contrast and visibility are highest when intensity of incident light on the display is lowest.

To view an EL display it is necessary to look through a transparent front electrode directly at the phosphor-dielectric and metal counter-electrode of the EL lamp capacitor structure. The light emitting phosphor-dielectric layer is also a strong diffuse reflector, so the same areas or patterns that are emitting light by electrical excitation are also reflecting about half of the incident light.

An EL phosphor powder and its embedding dielectric exhibit very little visible light absorption. As a result, they appear off-white in normal daylight or in artificial illumination. The effect of increasing the intensity of white light incident on an excited green display pattern is to reduce the green color saturation, making it progressively more white than green, until the eye can no longer discriminate any difference of color or intensity between the excited pattern and its background.

During recent years EL phosphor materials have been improved considerably in luminous efficiency and maximum attainable brightness. Although improvements in phosphors will always be needed and welcomed, the solution to the daylight visibility of EL cockpit displays cannot be found by merely increasing the brightness of light-emitting display patterns, for several reasons.

Observer fatigue is certainly a fundamental reason for not wanting to generate white displays with green emitting information patterns bright enough to be discerned in a high intensity daylight illumination environment.

Two other basic reasons ruling out the "brute force" approach are the increased electrical power dissipation and the loss in useful emission lifetime as EL phosphors are driven harder. Such limitations would contradict two of the more important basic development goals for solid-state displays.

During the course of this effort it has been proven that the only solution to such problems is to improve the optical design of the EL display lamp structure, so as to minimize these effects of incident light that cause loss of color and brightness contrast between the light-emitting information and its background. This means developing a lamp structure that will not only reduce the sources of reflection but also provide the maximum neutral density absorption of incident environmental illumination with the least absorption of display-emitted light. An EL display constructed to meet the above criterion will be called a "high-contrast EL display".

Figure 1 shows conventional and high-contrast EL numeric displays side by side under identical incident illumination. The numbers on the conventional display are actually about three times brighter than the numbers on the high contrast display, but their contrast is so low that they are barely discernible.

2. PRIOR STATE OF THE ART

Several contrast enhancing techniques were known at the start of this program. Some of these are:

- a. A perforated opaque overlay on the viewer side of the substrate to create an array of tiny viewing tunnels. In order to be effective, the viewing angle must be severely restricted.
- b. Use of a black dye in the phosphor-dielectric layer. Too much emitted light is absorbed relative to the incident light absorption.

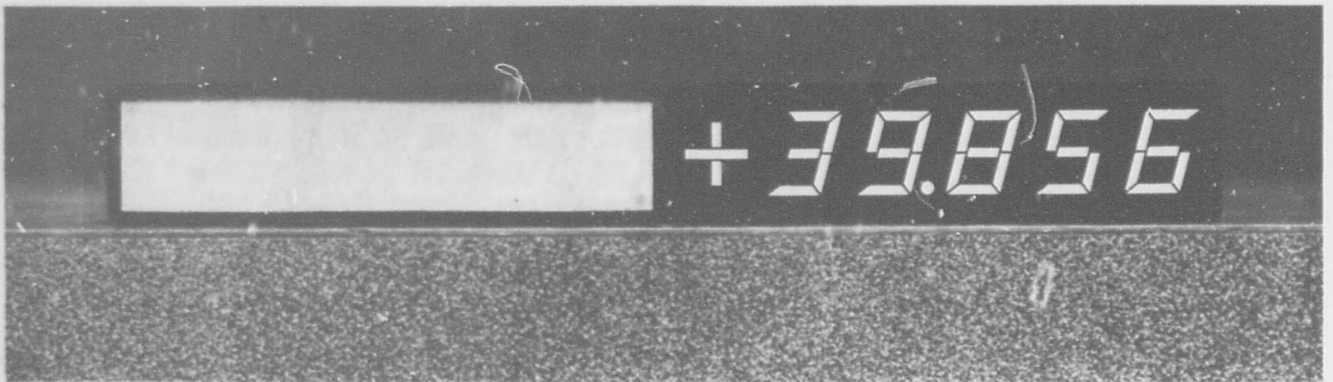


Figure 1. Conventional and High-Contrast EL Under Identical Incident Illumination

- c. Plastic absorption filter overlays, including polarizing filters. None of these have neutral density transmission, and interfacial reflections cannot be controlled.
- d. A "gray glass" substrate. Because it is not made in all thicknesses and optical densities, fabrication difficulties arise. Hiding power of reflection non-uniformities is poor.
- e. Use of vacuum-deposited thin film of a partially oxidized metal as a combination contrast filter and front electrode; however, specular reflectance is undesirably high.
- f. Opaque black particles uniformly distributed in a very thin dielectric layer located between the transparent front electrode and the phosphor-dielectric layer. This filter has neutral density transmission, superior hiding power, and complete fabrication versatility potentials.

The last two of these techniques originated at Lear Siegler and were the most attractive approaches. They were an inherent part of the lamp structure, and they allowed in-house control of light transmission and other characteristics.

Both of these techniques presented fabrication problems and were at least initially, very difficult to reproduce. It was not known whether they had durable enough mechanical characteristics to permit application in aircraft environments, and it was not clear why the opaque particle filter appeared to work better than other filters of the same percent light transmission.

SECTION II

SUMMARY OF RESULTS

1. GENERAL PRINCIPLE OF HIGH CONTRAST EL DISPLAYS

Since frequent use will be made of the term, "contrast ratio", and since the term evokes a variety of definitions, it is important to state now that by contrast ratio (CR) is meant:

$$CR = \frac{L_1 - L_0}{L_0}$$

where

L_1 = the luminance (emission plus reflectance) of an energized EL lamp segment

L_0 = the luminance of the background or unlit portion of the display

Maximum contrast ratio for any conditions of environmental illumination is the goal. It is obvious from the above expression that this goal would be achieved if the display had minimum reflectance, maximum absorption of incident light, and minimum absorption of light from phosphor emission. In addition, any segment or portion of the EL display, when not energized, must not be distinguishable from all the rest of the unlit areas of the display and its surrounding background. In other words, if none of the EL pattern is energized, it must not be possible to distinguish any pattern of reflectance non-uniformities, even with intense incident light.

The solution to these requirements is the insertion of some kind of low reflectance absorption filter between the diffuse reflecting phosphor-dielectric layer and the observer. The effect of this filter is to cause the incident environmental light to be doubly absorbed in the process of reflecting, while emitted light from the phosphor suffers only a single absorption.

Taking a specific example: 100% of incident light enters the EL display lamp structure; 30% emerges from the absorption filter, and 47% of this, or 14% of the total, returns from diffuse reflection off the phosphor-dielectric layer, only to be 70% absorbed during its second pass through the filter, leaving about 4% of the original incident light to be reflected to the observer. This is an oversimplified example that neglects, for the time being, interfacial reflection losses, specular reflection, angle of incidence, and electrical loss; it describes only the general condition of diffuse reflection.

If the above example is entered into the contrast ratio equation, and then compared to the case of the same display but without the absorption filter, the following results are obtained when the incident illumination is 1000 foot-candles and the phosphors are excited to emit 60 foot-lamberts:

$$\begin{aligned} \text{CR} &= 0.13 \text{ (no absorption filter)} \\ \text{CR} &= 0.43 \text{ (70\% absorbing filter)} \end{aligned}$$

Since it was assumed that both lamps had their phosphors excited equally, the luminance of the lamp with no filter was 3-1/3 times greater than the luminance of the lamp with the 70% absorbing filter. Just the reverse was true regarding their contrast ratios. The filtered lamp with 1/3 the luminance would require about 3.3 times the intensity of incident illumination to destroy the readability of the displayed information.

The last statement is true only if brightness contrast is considered. The filtered lamp has a greater color contrast than the conventional lamp, and eyes are more sensitive to color discrimination than to brightness discrimination. As a result, the improvement in readability of the filtered lamp will be greater than the preceding example indicates. This is illustrated later in the Human Factors section of this report.

2. PROGRAM ACCOMPLISHMENTS

A black appearing high-contrast filter with good hiding power was developed for EL displays. It consists of a uniform dispersion of opaque black particles suspended in a very thin transparent dielectric film, making a composite having neutral density light transmission, low reflectance, and high absorption efficiency.

In order to realize maximum benefit from potential color and brightness contrast provided by the filter, it was necessary to reduce to a minimum two interfacial specular reflections generated on the display substrate between the contrast filter and the observer. A three-layer optical interference film structure was found to be most satisfactory for the air-glass interface. The iridescent reflection from the glass-

transparent electrode interface was eliminated completely by increasing the optical thickness of the front electrode beyond the interference color range with an antireflection coating.

The EL lamp fabrication process was modified to incorporate both the contrast filter and internal antireflection coating, and good process control and reproducibility were developed. The resulting complex EL lamp structure can be temperature cycled between minus 55°C and plus 100°C without mechanical deterioration.

Special hard pads were developed to prevent contrast filter damage caused by pressure contacts deforming the EL layers during high temperature storage. They are fabricated as an integral part of the rear electrode configuration.

A method was developed for displaying complex static patterns, such as words, without having to segment the electrodes or alter the completely uniform transmission and absorption of the contrast filter.

The human factors study and Air Force flight test evaluations revealed the importance of secondary reflections in the viewing environment. The ability of the front air-glass interface of a high contrast EL display to reflect confusing images back to the observer was minimized by using antireflection coatings and eliminated where practical by control of the spectral source. The useful visibility of improved high-contrast EL displays in daylight cockpit conditions was demonstrated in flight tests as well as in the Terradyne simulator used for the human factors study.

A large, relatively complex EL display format of an experimental altimeter was built to demonstrate all of the advances in high-contrast EL display techniques that were developed during the course of this program. The display, which used green and amber EL phosphors, had a format which was partly active and partly static. The active sections were the bar graph, and two small seven-stroke numerics. Figure 2 shows the interior of the display's metal case next to the EL substrate with its rear electrode side showing. Figure 3 shows the assembled display in both the "off" and "on" states.

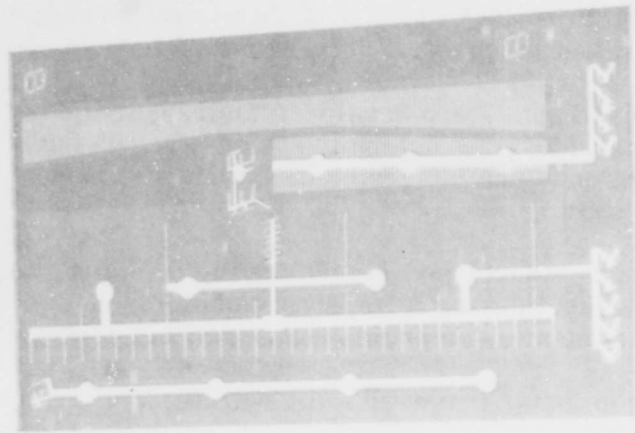
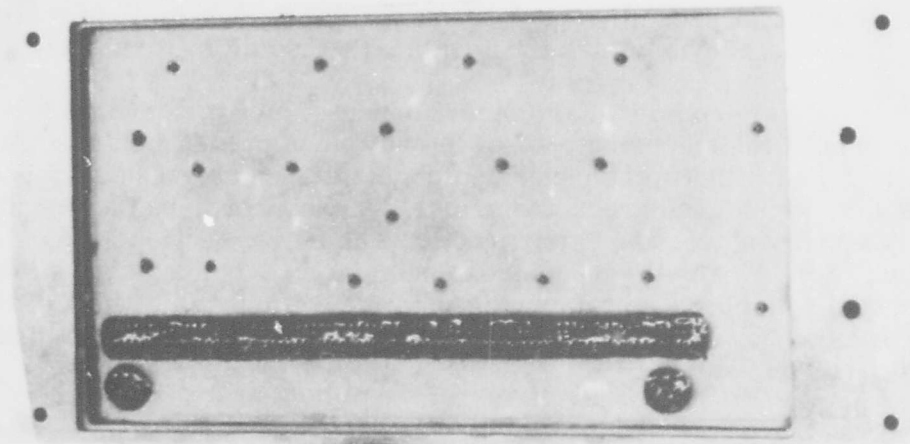


Figure 2. Experimental Altimeter Display Before Assembly

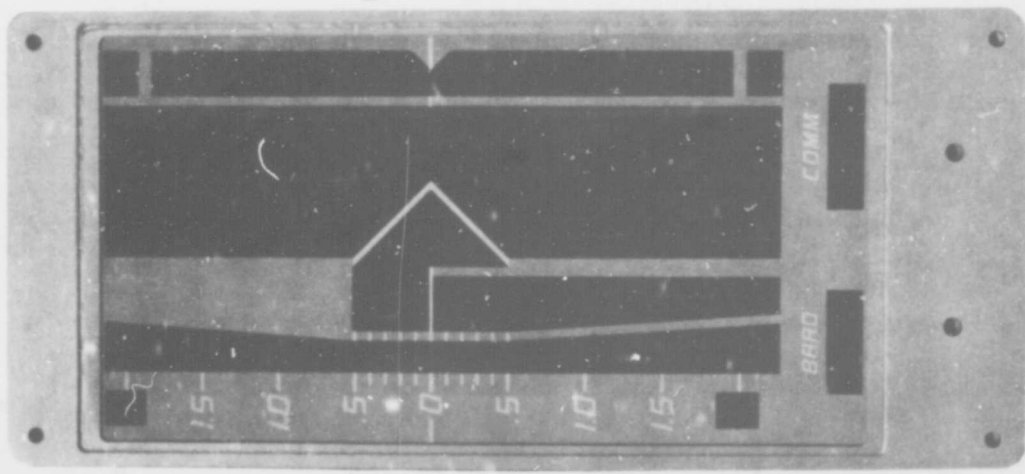
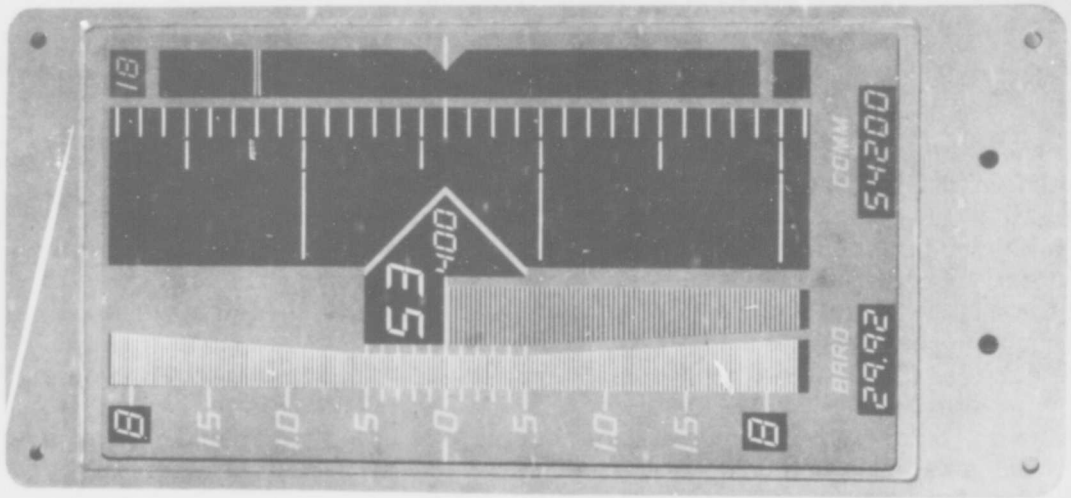


Figure 3. Experimental Altimeter Display After Assembly

SECTION III

TECHNIQUE DEVELOPMENT

During the early stages of contrast filter development, both the vacuum-deposited, partially oxidized metal filter and the opaque particle filter were investigated. The vacuum-deposited filter was improved by addition of an oxide optical interference film to render its dark gray specular reflection dark blue-violet. Additionally, the substrate was etched prior to film deposition in order to diffuse its reflectance. In spite of these efforts and improvements, the vacuum-deposited filter had substantially higher total reflectance than the opaque particle filter, and the process for making it was becoming too complex.

Progress on the particle filter was rapid during this same time, and its appearance was consistently better. As a result, the vacuum-deposited filter was dropped, so that more effort could be devoted to the more promising particle filter.

The bulk of this report will be devoted to the opaque particle filter, and it will simply be referred to as the "high-contrast filter" or "contrast filter".

1. OPTICAL CONSIDERATIONS

a. Reflections and Their Sources

One of the primary problems in the development of an electro-luminescent display panel with an improved contrast ratio is the reflection of ambient light from the various surfaces. The normal EL lamp without a high contrast layer has four sources of reflection:

- (1) The front surface reflection of the glass substrate.
- (2) The glass-NESA* interface.
- (3) The interface between the Nesa film and the phosphor-dielectric layer.
- (4) The interface between the phosphor-dielectric layer and the rear dielectric or back electrode configuration.

*NESA is a trade name for a transparent, electrically conductive thin film of tin oxide.

The equations for reflection of electro-magnetic radiation are well known, and a comprehensive discussion can be found in any text-book on physical optics. Some of the important results will be stated and applied to this EL panel configuration.

Maxwell's equations of the electromagnetic field have been applied to the boundary between a material and the surrounding medium to derive the laws of reflection for a plane surface, with the following results:

$$\rho_{\parallel} = \frac{\tan^2(\theta - \phi)}{\tan^2(\theta + \phi)}, \quad \rho_{\perp} = \frac{\sin^2(\theta - \phi)}{\sin^2(\theta + \phi)} \quad (1)$$

where

θ = angle of incidence

ϕ = angle of refraction

ρ_{\parallel} = reflectance for parallel polarized radiation.

ρ_{\perp} = reflectance for perpendicularly polarized radiation.

These equations were first derived by Fresnel and are known as Fresnel's laws of reflection.

The angles, θ and ϕ , are related by Snell's law:

$$\sin \phi = \frac{\eta_1}{\eta_2} \sin \theta \quad (2)$$

where

η_1 = index of refraction of the material.

η_2 = index of refraction of the surrounding medium.

For many materials, the index of refraction is complex with the imaginary part being proportional to the absorbing characteristics of the material.

The complex index of refraction, η_1 , is written as

$$\eta' = \eta - iK \quad (3)$$

where

K = absorption index

η = real part of the refractive index

The absorption index and absorption coefficient are related as follows:

$$K = \frac{\alpha \lambda}{4 \pi} \quad (4)$$

where

α = absorption coefficient

λ = wavelength

Using Snell's law, Fresnel's equation can be rewritten:

$$P_{11} = \left[\frac{\cos \theta - \sqrt{\left(\frac{\eta_2}{\eta_1}\right)^2 - \sin^2 \theta}}{\cos \theta + \sqrt{\left(\frac{\eta_2}{\eta_1}\right)^2 - \sin^2 \theta}} \right]^2 \quad (5)$$

$$P_{\perp} = \left[\frac{\left(\frac{\eta_2}{\eta_1}\right)^2 \cos \theta - \sqrt{\left(\frac{\eta_2}{\eta_1}\right)^2 - \sin^2 \theta}}{\left(\frac{\eta_2}{\eta_1}\right)^2 \cos \theta + \sqrt{\left(\frac{\eta_2}{\eta_1}\right)^2 - \sin^2 \theta}} \right]^2 \quad (6)$$

For perpendicular incidence ($\theta = 0^\circ$), the relation between reflectance, ρ_0 , and the indices of refraction η_1 and η_2 is simple:

$$\rho_0 = \rho_{11} = \rho_{\perp} = \frac{(\eta_2 - \eta_1)^2}{(\eta_2 + \eta_1)^2} \quad (7)$$

For unpolarized incident light, the reflectance, ρ , is simply the average of ρ_{11} and ρ_{\perp} :

$$\rho = 1/2 (\rho_{11} + \rho_{\perp})$$

Applying these principles to the air-glass interface of the EL display panel will give the reflection factors shown in Table I. The index of refraction of the glass substrate is 1.50. Also given are the values of ρ_{11} and ρ_{\perp} for various angles of incidence. As well as the reflection factor for unpolarized light at various angles of incidence.

These principles can also be applied to the interface between the glass substrate and NESA film to give Table II. The index of refraction of the Nesa film is assumed to be 2.0.

Shown in the tables are values of θ at which ρ_{11} is equal to zero. This angle is known as the polarizing angle, or the principle angle of incidence, for which the reflected light is all plane-polarized with the electric vector perpendicular to the plane of incidence.

Table I. Reflection Factors for Air-Glass Interface for Various Angles of Incidence

θ	0°	15°	30°	45°	53.3°	60°	75°	90°
ρ_{\perp}	.040	.044	.058	.092	.148	.177	.399	1.000
ρ_{11}	.040	.036	.025	.008	.000	.002	.107	1.000
ρ_{θ}	.040	.040	.0415	.050	.074	.0895	.253	1.000

Table II. Reflection Factors for Glass NESA Film Interface for Various Angles of Incidence

θ	=	0°	15°	30°	45°	53°	60°	75°	90°
ρ_{\perp}	=	.020	.023	.032	.053	.079	.111	.316	1.000
ρ_{\parallel}	=	.020	.018	.012	.003	0	.003	.110	1.000
ρ_{θ}	=	.020	.020	.022	.028	.040	.057	.213	1.000

The previous discussion is concerned primarily with the concept of specular reflection. The variation of the reflectance, ρ_{θ} , is small for angles of incidence below the polarizing angle but rapidly increases as the angle of incidence becomes larger.

Another situation to consider is that of perfectly diffuse ambient light. In this case light incident at all angles is illuminating the surface of the display. The reflection factor of a plane boundary between two media is computed by the Fresnel formula as a function of the relative index of refraction, $N = \eta_2/\eta_1$, of the media.

The average value of the external reflection coefficient is:

$$\rho_e = 2 \int_0^{\pi/2} \rho_{\theta} \sin \theta \cos \theta d\theta \quad (8)$$

where ρ_{θ} is the reflectance by the Fresnel formula for unpolarized light incident on the surface from the rarer medium at an angle, θ .

If the diffuse light is incident on an interface from the denser medium the reflection factor will be considerably different from that for external reflection.

There is an important optical relation that permits easy evaluation of this internal reflection. This is the reciprocal relation which states that all changes suffered by a light beam going in one direction are

suffered equally by a light beam formed by reversing the direction of the first. Using this relation and previous notation, the angle ϕ is now the angle of incidence in the dense medium and θ is the angle of refraction in the rare medium. The diffuse light will be incident on the interface at all angles, ϕ . Snell's law shows that -

$$\sin \phi = \frac{\eta_1}{\eta_2} \sin \theta \quad (9)$$

If θ , the angle of refraction, is equal to 90° then $\sin \theta = 1$. Therefore, at this angle, $\sin \theta_c = \eta_1/\eta_2$. The light beam incident at this angle is bent parallel to the interface and does not penetrate into the less dense medium. Any light incident at greater angles is totally reflected. This angle, θ_c , is known as the critical angle; for the glass-air and the NESA-glass interfaces, the angles are 42° and 48.5° , respectively.

The reflection coefficient for diffused light incident from the dense to the rarer medium can be evaluated from the following equation:

$$\rho_i = (1 - \sin^2 \phi_c) + 2 \int_0^{\pi/2} \rho_\phi \sin \phi \cos \phi d\phi \quad (10)$$

where

ρ_ϕ = the reflectance by the Fresnel formula for unpolarized light incident on the surface from the denser medium at angle, ϕ , from the perpendicular to the surface

ϕ_c = the critical angle.

Figure 4 shows the average reflection coefficient, ρ_i , as a function of the refractive index ratio, η_2/η_1 . For comparison, it also shows the average external reflection, ρ_e , as well as the reflectance ρ_o for perpendicular incidence. It is seen from Figure 4 that approximately 9% of the incident perfectly diffuse light is

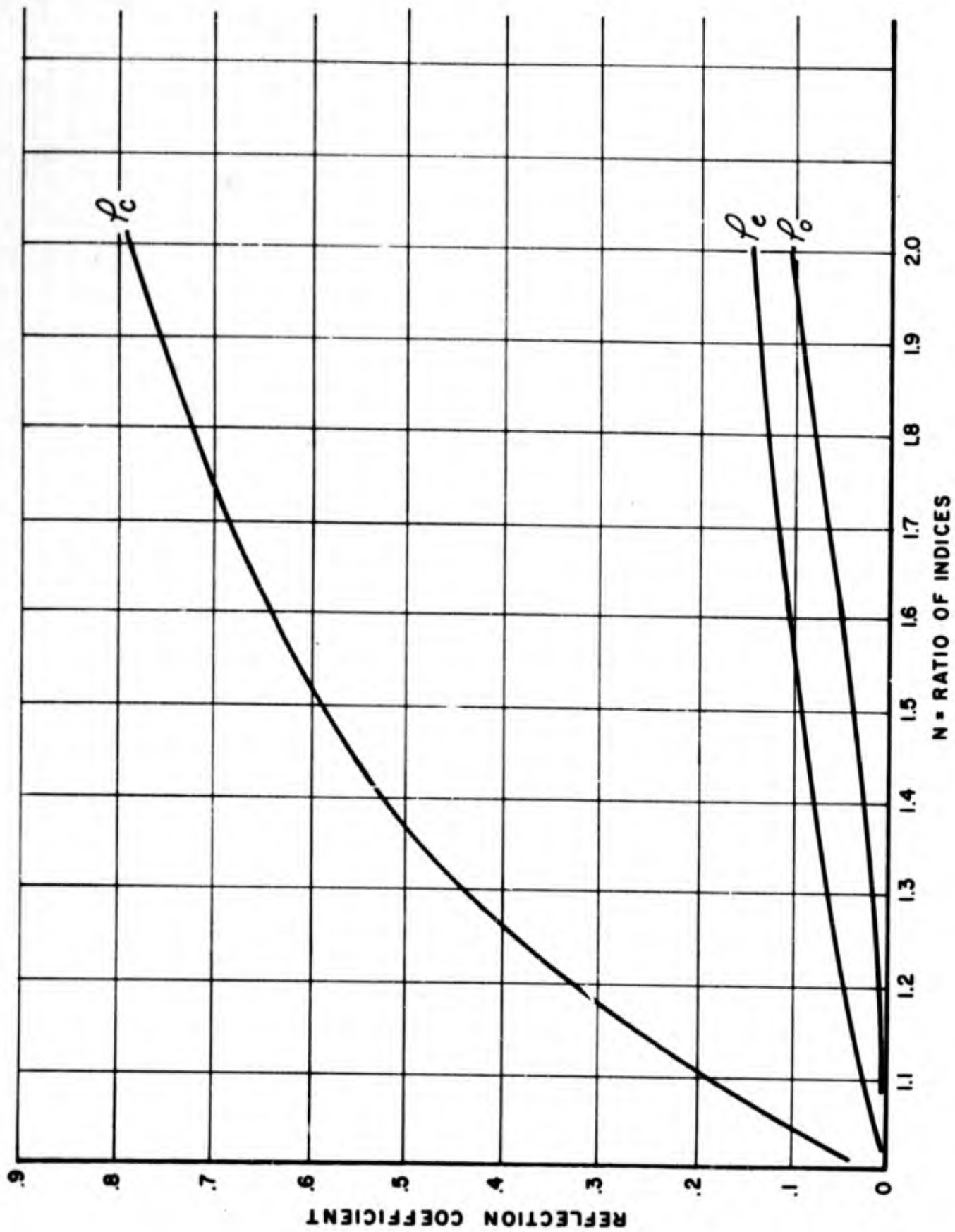


Figure 4. Reflection Coefficients Vs. Ratio of Indices

reflected from the air-glass interface. Further, nearly 60% of the diffuse-flux incident internally is reflected; little more than 40% emerges. For the glass-NESA interface, the total external reflectance is 6.5%. The glass-NESA interface will reflect 47% and transmit 53% of internally incident light.

The reflection of light from the phosphor-dielectric layer is not easily treated. In this case the optical medium is composed of EL particles embedded in a dielectric medium.

Consider now what happens when the refracted beam meets a phosphor particle.

If the particle, or cluster of particles, has dimensions larger by a factor of about 10 than the wavelength of the light, part of the flux of the incident beam will be reflected and part refracted again in accord with Fresnel's equations. But, since the randomly oriented phosphor particles present faces at unknown angles to the refracted beam, the identity of the beam is lost at this point. Part of it is reflected, part penetrates the phosphor particles and emerges modified in spectral character by any selective absorption within the phosphor particles. These parts go on in random courses striking other phosphor particles. The net effect is a diffusion of flux more or less uniform in all directions at any point in the phosphor-dielectric layer.

If the phosphor particles are considerably smaller in dimensions than the wavelength of the incident energy, the Fresnel laws do not apply. As the particle sizes become smaller, the light begins to go around the particle in addition to reflection and refraction. In this process, some of the flux is absorbed and the rest is scattered, some backward, some to the sides, but mostly in the forward direction. The laws of scattering are quite complicated and will not be discussed in any great detail at this point. The phenomena of scattering are discussed in the Appendix and will be applied in more detail to the absorption layer used to achieve a high-contrast EL display.

As pointed out in the Appendix, the extent of the scattering is determined primarily by the size of the particles and by the ratio of the index of refraction of the phosphor particles to that of the dielectric medium. There is a range of phosphor particle sizes in the EL layer; about 95% fall between 2 and 20 microns. Also, as the ratio of indices is large, the phosphor-dielectric layer is an excellent scattering agent. It is difficult to predict the reflectance factors since it is highly dependent on both the particle size and particle density.

Some idea of the magnitudes involved can be derived from our previous discussion on reflection of diffused light. Figure 4 shows that for a ratio of indices of 1.6, approximately 10% of the externally incident light is reflected from the surface of the phosphor-dielectric layer. The flux penetrating the upper boundary of the layer is diffused more or less uniformly in all directions. Some of this diffuse flux is reflected back towards the upper boundary from the particles in the layer. Since this flux is internally incident, only 35% penetrates through the upper boundary and 65% is reflected back into the layer. Obviously, the flux suffers successive reflections similar to that observed in a medium bounded by two parallel planar boundaries.

The flux which does pass through the phosphor-dielectric layer reaches the reflecting surface formed by the phosphor-dielectric layer and the back electrode configuration. This surface reflection will also contribute to the total reflectance.

b. Methods for Reducing Reflections

As pointed out in the previous section, most of the reflection observed on a normal EL lamp is due to reflections from the interfaces formed by the front and back surfaces of the phosphor-dielectric layer.

A promising technique for reducing these reflections is to insert neutral density filter of low reflectance between the transparent front electrode and the phosphor-dielectric layer. The optical requirements of this layer have been considered in some detail. The layer, as prepared, is a dielectric medium containing uniformly dispersed opaque particles; it has a top surface, a bottom surface, and an interior whose thickness is small compared to its length and width. A portion of the light flux incident on the top surface is reflected without penetrating the film. Some of the incident light flux penetrates the surface and, is absorbed there. The rest is either scattered back out through the top surface or reaches the bottom surface where it is reflected from the phosphor-dielectric layer. The power of the absorbing layer to absorb and diffuse the light flux penetrating it determines whether the underlying phosphor-dielectric layer is or is not visible to the viewer. This is known as opacity or hiding power.

Obviously there is no interest in a completely opaque film, since it is still necessary that the EL segments be visible when activated.

The function of the absorbing film, therefore, is to reduce the total amount of ambient light striking the light-colored, reflecting phosphor particles, and then to further attenuate this light after it reflects off the phosphor. The ambient light is at least doubly absorbed whereas the phosphor's emitted light is absorbed only once -- this results in an increased contrast between the emitting display and its adjacent background.

The capacity of the absorbing layer to hide the light-colored phosphor layer is dependent chiefly on the number and size of opaque particles per unit area and on their light-absorbing and light-scattering capacity.

Studies of the scattering and absorption of light in a heterogeneous material can be categorized into two basic areas: 1) scattering and absorption by individual particles and 2) multiple scattering in a medium containing many scattering particles. The first area concerns the definition of the scattering and absorption coefficients of a single particle from a knowledge of its geometry and physical properties and the characteristics of the incident light. The theoretical characteristics of a particle involves obtaining a solution to the Maxwell equations for the interaction between the electromagnetic radiation and the particle. The rigorous formulation applicable to particles of arbitrary size and for spherical particles is known as the Mie theory of particle scattering. The formulae of the Mie theory are described in the Appendix.

The second area concerns the definition of radiative transfer within and from a scattering system. Differential equations describing the radiant flux are formulated in terms of "apparent" absorption and scattering coefficients. The radiative-transfer equations are thus seen to do nothing toward predicting the absorption and scattering coefficients, but predict system performance once these coefficients are known.

The absorption and scattering coefficients employed by the one-dimensional radiative-transfer equations are related to, but not equal to, the coefficients defined by single particle theory. The theory of single scattering by independent particles breaks down when particles are brought into close proximity. The precise conditions implied by the theory are that each particle must have sufficient room to form its own scattering pattern without interference from neighboring particles, and that each particle must be exposed to the original beam of incident light.

In this case, the multiple scattering taking place makes it impossible to quantitatively analyze the neutral density filter. Using some of the information available from single-particle theory does allow the choice of materials with promising optical characteristics.

The most important optical characteristics which must be considered in the single-particle theory are particle size, index of refraction, particle shape, and orientation.

The quantities of primary interest for application to the problem are parameters specifying the fraction of the energy incident on a particle that is scattered and absorbed. The quantities Q_{ext} , Q_{sc} , and Q_{abs} are defined in the Appendix. These are the efficiency factors for extinction, scattering, and absorption, respectively. Another quantity of interest is the ratio of backscattering ($\theta = 0^\circ$) to forward scattering ($\theta = 180^\circ$). This ratio will give some indication of the amount of light reflected toward the observer. The efficiency factor and scattering ratio are affected primarily by the ratio of the particle size to the wave-length of the incident radiation and by the index of refraction of the particle relative to the index of refraction of the surrounding medium.

In discussing extinction, scattering and absorption factors, it will be helpful to employ the particle size factor, x , defined in the Appendix,

$$\left(x = \frac{2 \pi r}{\lambda_m} \right)$$

In order to obtain some insight into the effects of particle size and index of refraction on these factors, a program was prepared for the IBM 360 in the Lear Siegler Computing Center. Representative values of the index of refraction and particle size were inserted into the program, Figures 5, 6 and 7 are typical examples of the results obtained from these computations.

When the particle size is small relative to the wavelength, the domain of Rayleigh scattering is encountered. Scattering efficiency is very low and proportional to the fourth power of the ratio of particle size to wavelength. In the Rayleigh domain, an isotropic particle has a backscatter ratio of 0.5 for incident unpolarized light.

As the particle size is increased, the scattering efficiency continues to increase, but the rate of increase is diminished from a fourth-power

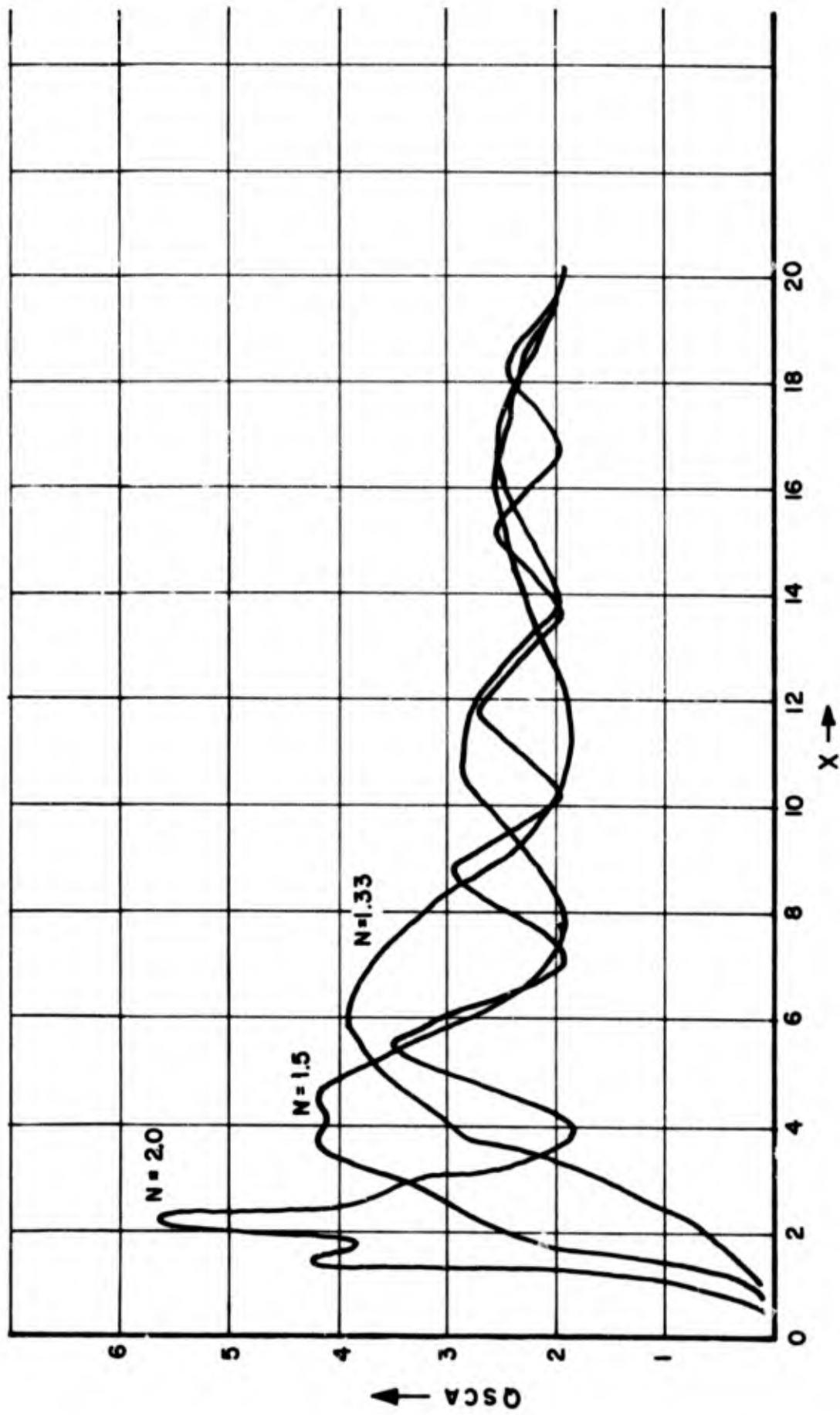


Figure 5. Scattering Efficiency Vs. Size Factor for Various Ratios of Indices

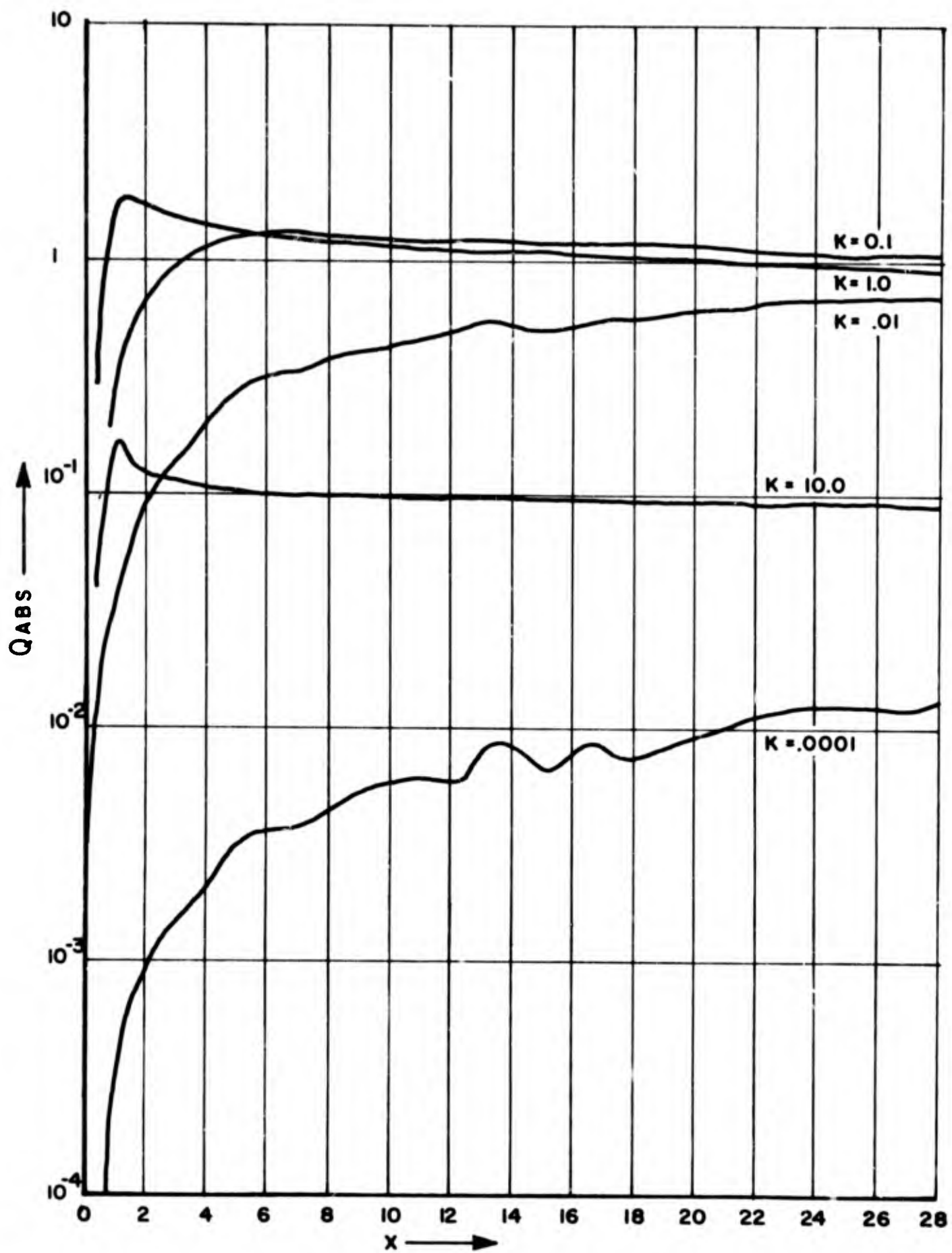


Figure 6. Efficiency Factor for Absorption as a Function of X, the Particle Size Factor and the Absorption Coefficient, K. ($N = 1.5 - iK$)

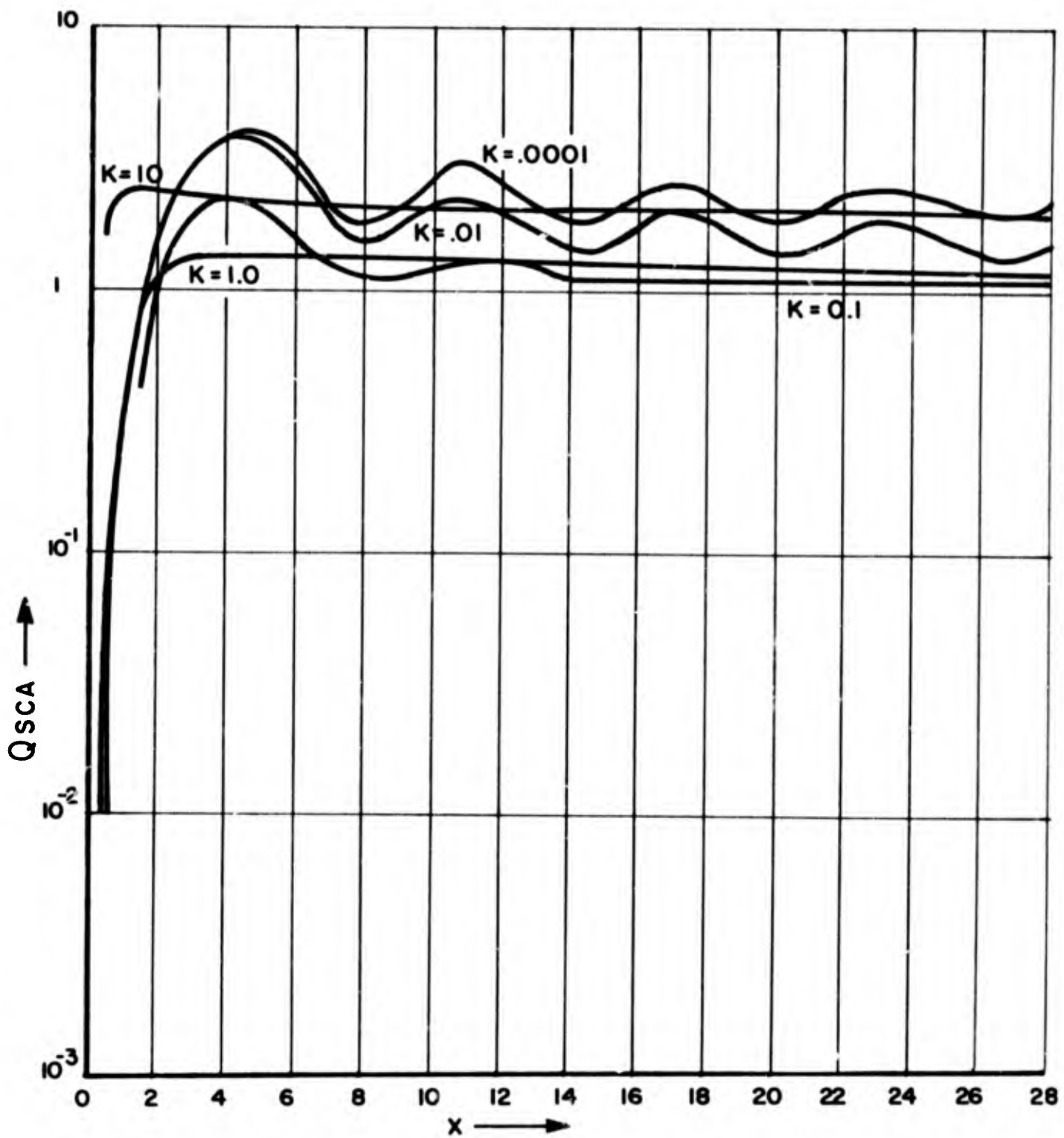


Figure 7. Efficiency Factor for Scattering as a Function of X , the Particle Size Factor and the Absorption Coefficient, K . ($N = 1.5 - iK$)

dependence on particle size to a second-power dependence. This region is known as the Rayleigh-Gans domain. As particle size is increased in this domain, the backscatter ratio decreases from 0.5 to lower values, continually decreasing as the particles are made larger. Most of the scattering now take place in the forward direction.

A further increase in particle size places the scattering in the range where so-called Mie scattering takes place. The physical effect now becomes one of interference between transmitted radiation and diffracted radiation. As particle size is increased in this region, scattering efficiency continues to increase until a maximum efficiency is reached at a particular particle size. From the curves for efficiency factors, it can be seen that generally the most efficient scatterer is a particle whose diameter is of the order of the wavelength of incident light. At this point there is a favorable interference between the various wave fronts involved. Still larger particle sizes result in unfavorable interference and the scattering efficiency decreases. A pattern of maxima and minima occurs as the particle size is continually increased. The complete curve oscillates with a decreasing amplitude about an efficiency value of 2.

In the upper limit of the anomolous-diffraction domain, interference effects diminish and the scattered radiation can be separated into two components. The first component is radiation transmitted essentially according to the laws of geometric optics.

The second component is radiation diffracted around the particle. The sum of the two is equal to twice the geometric area of the particle so that

$$Q_{\text{ext}} = \frac{\sigma_{\text{ext}}}{\pi r^2} = \frac{2 \pi r^2}{\pi r^2} = 2$$

Throughout the anomolous-diffraction domain, scattering remains predominantly in the forward direction.

Another important optical characteristic which was examined was the refractive index and its influence on efficiency and back-scattering. Of particular interest is the index of refraction of the scattering particle as well as the ratio of the indices of the particles and embedding medium. Figure 5 indicates the effects of varying the ratio of indices. Scattering efficiency increases with increasing N. The backscatter ratio also increases with increasing N. It was

mentioned earlier that for a fixed index ratio, the backscatter ratio decreased as the particle size was increased. It can now be seen that if the particle size is fixed and the index ratio is increased, the backscatter ratio is increased.

A layer with non-absorbing particles does not necessarily give a desirable filter. It is true that the backscatter from the layer may be reduced to a low value, but most of the incident light flux will be scattered in the forward direction where it will reach the phosphor layer and, in turn, be reflected back through the filter. This light flux will, in turn, be scattered primarily in the forward direction back towards the observer. The filter, therefore, must also contain highly absorbing particles which will tend to absorb most of the scattered light.

As pointed out in the Appendix, direct absorption is defined in terms of efficiency factor Q_{abs} . The absorption index will also have an effect on the efficiency factor for scattering. Figures 6 and 7 were plotted to show the effect of increasing absorption index on these two efficiency factors. These show that the dominant effect of the absorption index is to reduce the scattering efficiency of the layer. This is desirable in this filter in order to reduce the magnitude of the backscattering. It is also quite obvious from these curves that particle size has very little effect when the absorption index is large.

When the concentration of the particles in the layer is large (as in this filter), multiple scattering occurs. The problem of analysis becomes extremely difficult and the results discussed above can be used only as a guideline to choose promising materials and particle concentrations for the filter. Some attempts have been made in the literature to study multiple scattering systems, but they leave a lot to be desired.

The above single particle characteristics, therefore, were used as guidelines to develop the absorption filter used in the high-contrast EL lamp. LSI found these guidelines to be of extreme usefulness in this program.

Specular reflection from the front glass surface of the EL display can also cause considerable trouble. This type of reflection can be reduced by applying antireflection coatings to the glass surface.

There are several methods which can be used to produce such coatings. Since there are several types available commercially most of the work was concerned with testing the various coatings in finished EL samples.

2. TECHNIQUES AND MEASUREMENTS

a. Measuring Techniques

Reflection measurements were made with simple set-ups using a MgO block as a standard. A light source was mounted on a movable arm which allowed the angle of incidence to be varied. The reflecting surface was mounted on a rotating table which permitted the viewing angle to be varied. This arrangement made it possible to study the front surface reflections in detail.

Also available was a test set-up which used a ring-shaped fluorescent tube as a light source. This tube was centered around an axial line from the photometer to the sample. The fluorescent tube was positioned to give an illuminance of 300 foot-candles on a surface placed at the sample position.

Luminance and luminance factors were measured with photo-multiplier photometers.

Typical diffuse reflectance curves for a MgO surface are shown in Figures 8 and 9. Curves were obtained for the light source at various angles, but most measurements were made at the angles, $\theta = 0^\circ$ and $\theta = 45^\circ$.

b. Contrast Filter Measurements

Figures 10 and 11 are directional reflectances for conventional EL lamps. As indicated on the curves, each is for a different type of phosphor. The curves show that nearly 50% of the incident light is reflected from the lamp. Further, the directional reflectance from the front surface of the lamp is extremely high when the viewing angle is equal to the angle of incidence. This indicates that any images formed on the front surfaces will give extremely high directional reflectance. The phosphor layer itself is a very good diffusing surface as indicated by the curves obtained with the light source normal to the lamps. Although not obvious from these curves, other data indicate that there is some variation in diffuse reflectance with the type of phosphor used. This is due to both a variation in particle size and index of refraction.

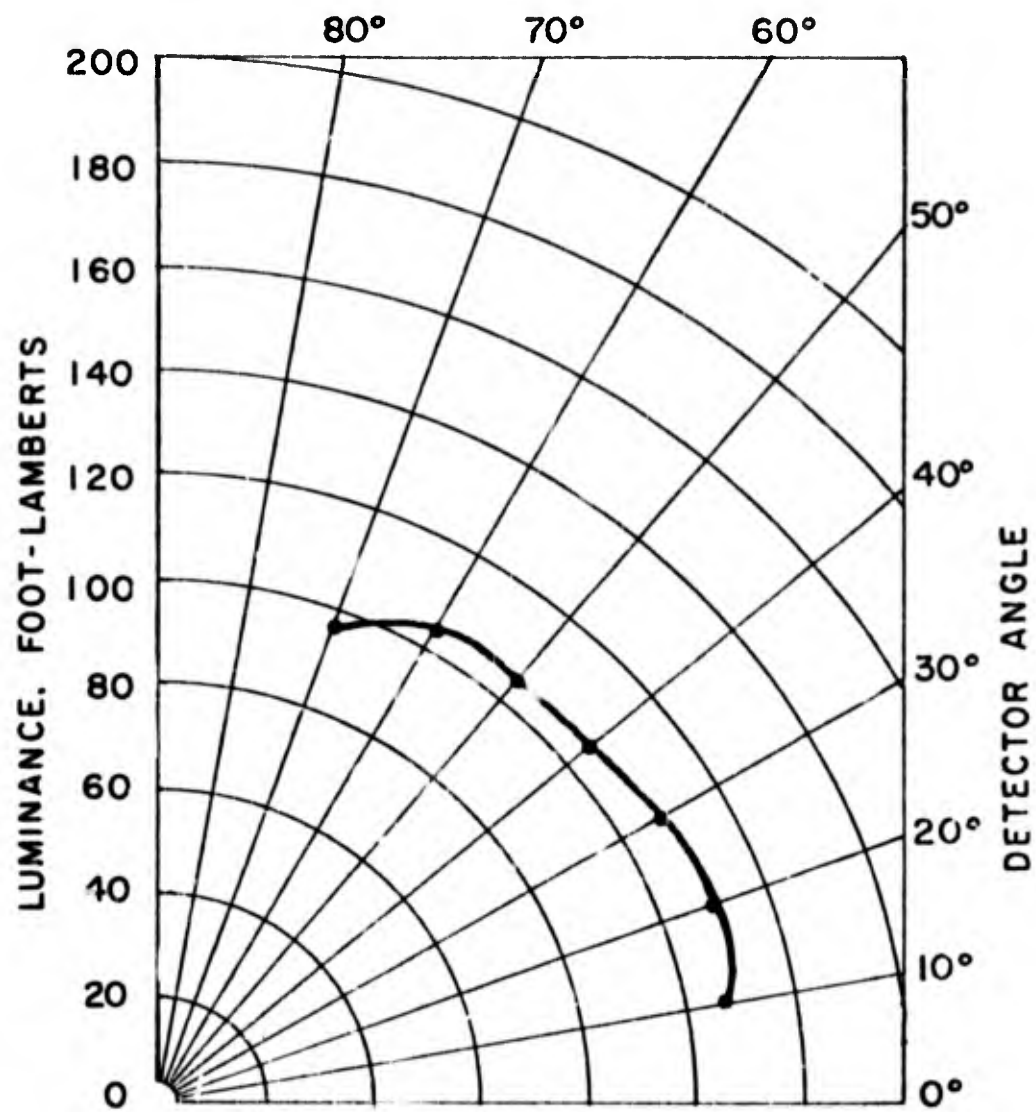


Figure 8. White Diffuse Standard (98% Reflectance)
Light Source Normal to Surface

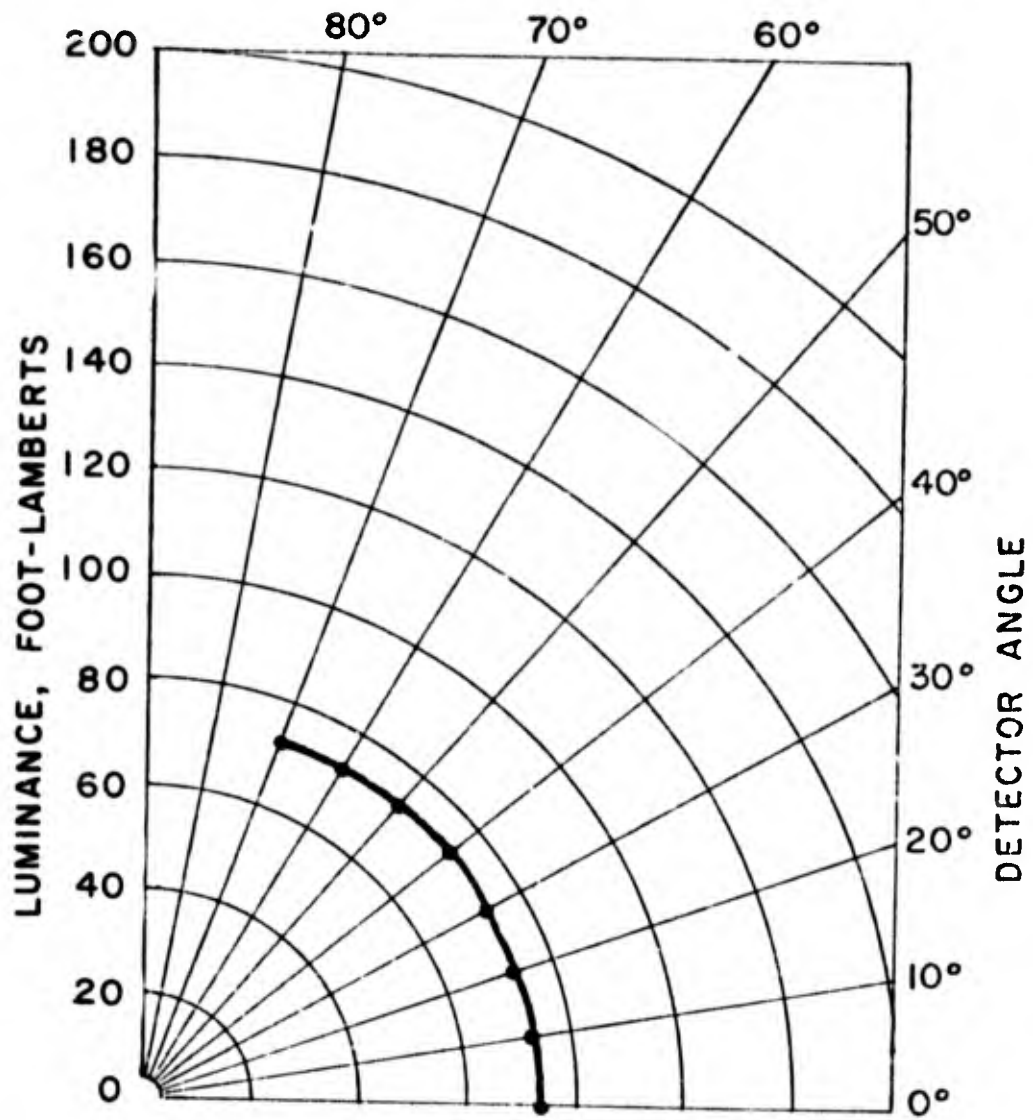


Figure 9. White Diffuse Standard (98% Reflectance)
 Light Source 45° From Normal to Surface

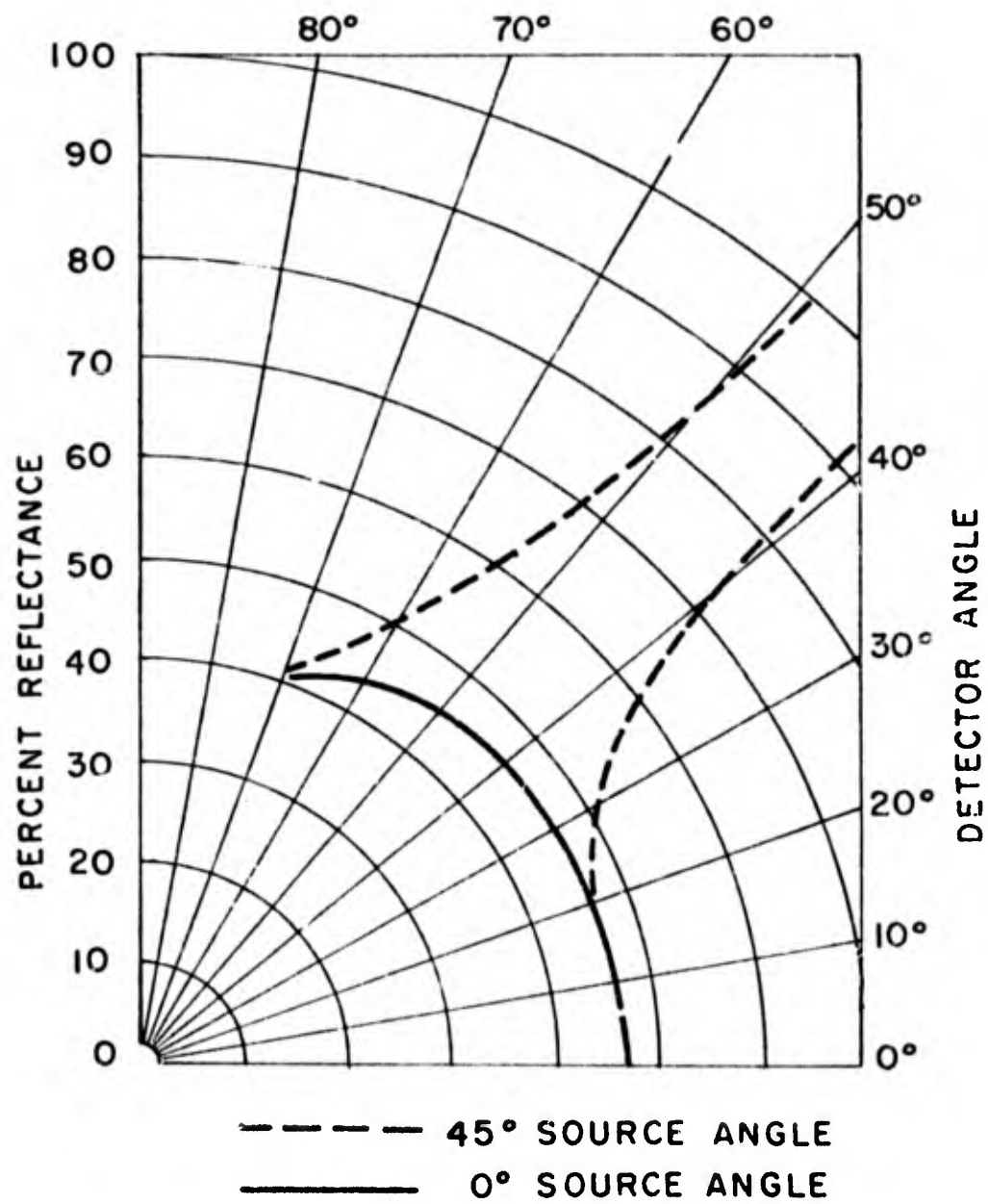


Figure 10. Percent Reflectance of Conventional EL Lamp

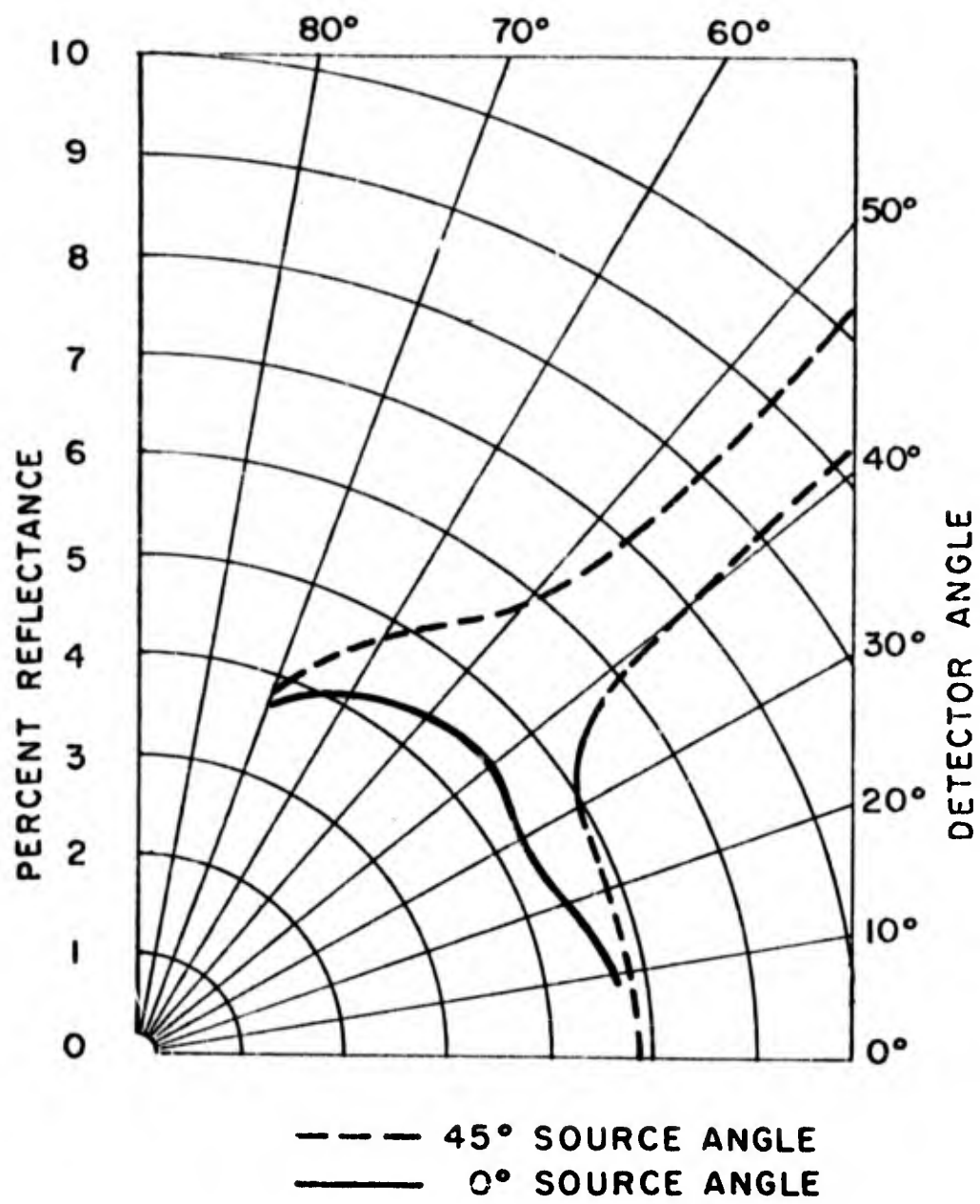


Figure 11. Percent Reflectance of Conventional EL Lamp

Samples were prepared which enabled us to measure the reflectances from the various surfaces present in the EL display. Measurements were made in the test set-up using a fluorescent light source. The diffuse reflectance of the rear dielectric layer on an aluminum surface ranged between 60 and 70%. The diffuse reflectances of phosphor layers on black opaque substrates typically fell between 45 and 50%, while that of phosphor layers sprayed on rear dielectric layers ranged from 60 to 65%. The directional reflectance of the glass-NESA combination varies from 10 to 15%. Variations in the optical thickness and refractive index of the tin oxide film (NESA) caused this latter variation.

Some of the above test chips were sprayed with contrast filters which had a transmission of 30%. The diffuse reflectances of these samples were reduced to values less than 8%.

Additional measurements were also made in the variable test set-up. Typical results obtained for samples similar to those above are shown in Figures 12 and 13. The sample in Figure 12 consists of a phosphor layer and contrast filter over a black opaque substrate. In Figure 13 the sample has a rear dielectric layer between the phosphor and black, opaque substrate. The curves indicate that, although there is a 15% difference in diffuse reflectance from the two samples, the reflectance factors for the contrast filter surface are approximately the same.

The curves obtained for the light source at 45° show that the contrast filter absorbs and scatters the incident light. The reflectance, with the light source normal to the filter surface, is a maximum in the back direction. With the light source at 45° from the normal, the reflectance keeps increasing as the angle of view increases. This result, in particular, indicates that scattering of the incident light does occur at the filter surface.

Figure 14 shows transmission curves obtained for a 30% transmitting contrast filter for the incident light normal to the surface and 45° from the normal. In both cases, maximum transmission occurs in the direction of incident light. The particle size is such that light is predominantly scattered in the forward direction.

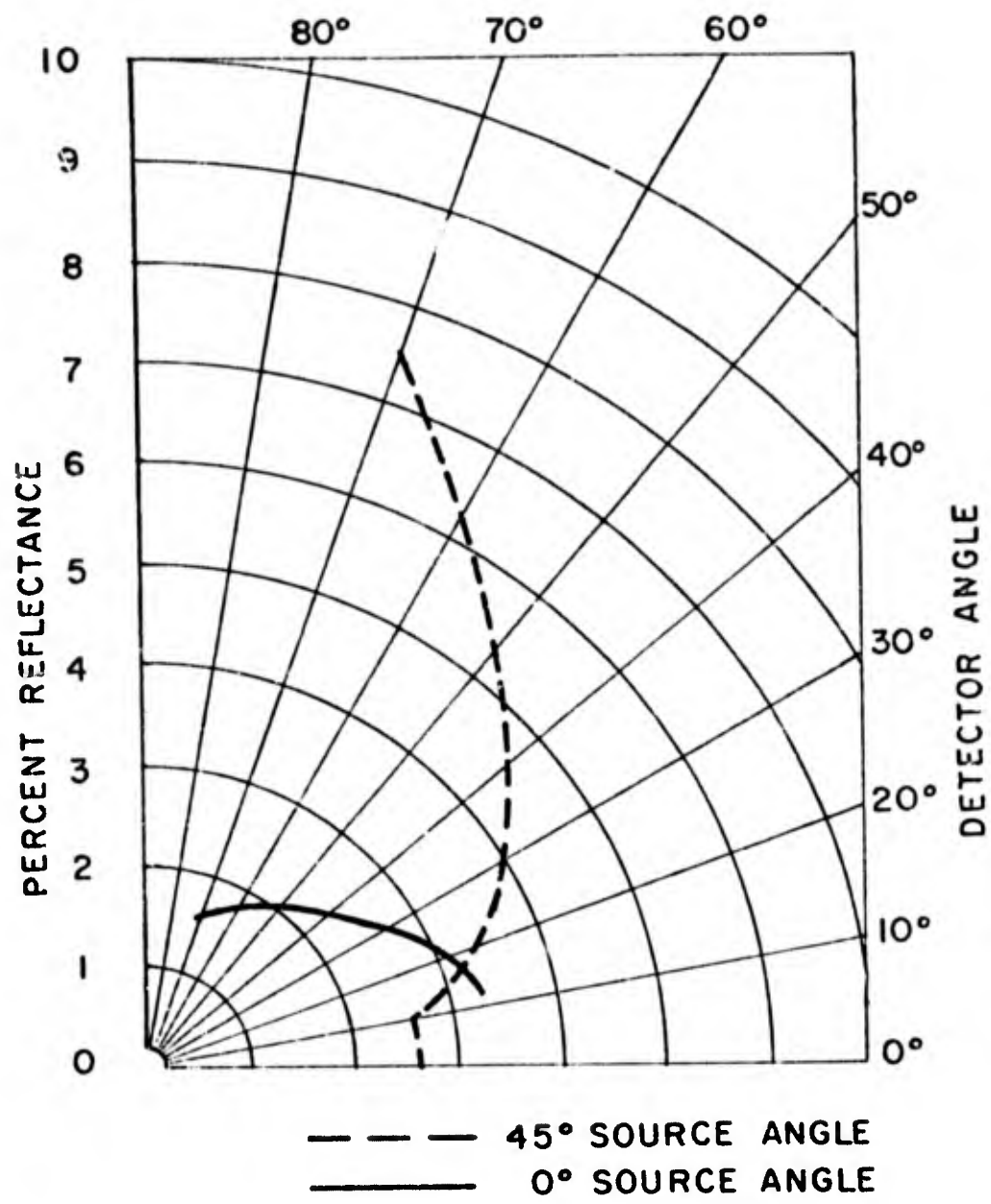


Figure 12. Percent Reflectance From Surface of High-Contrast Layer With No Insulating Layer Behind the High-Contrast Layer

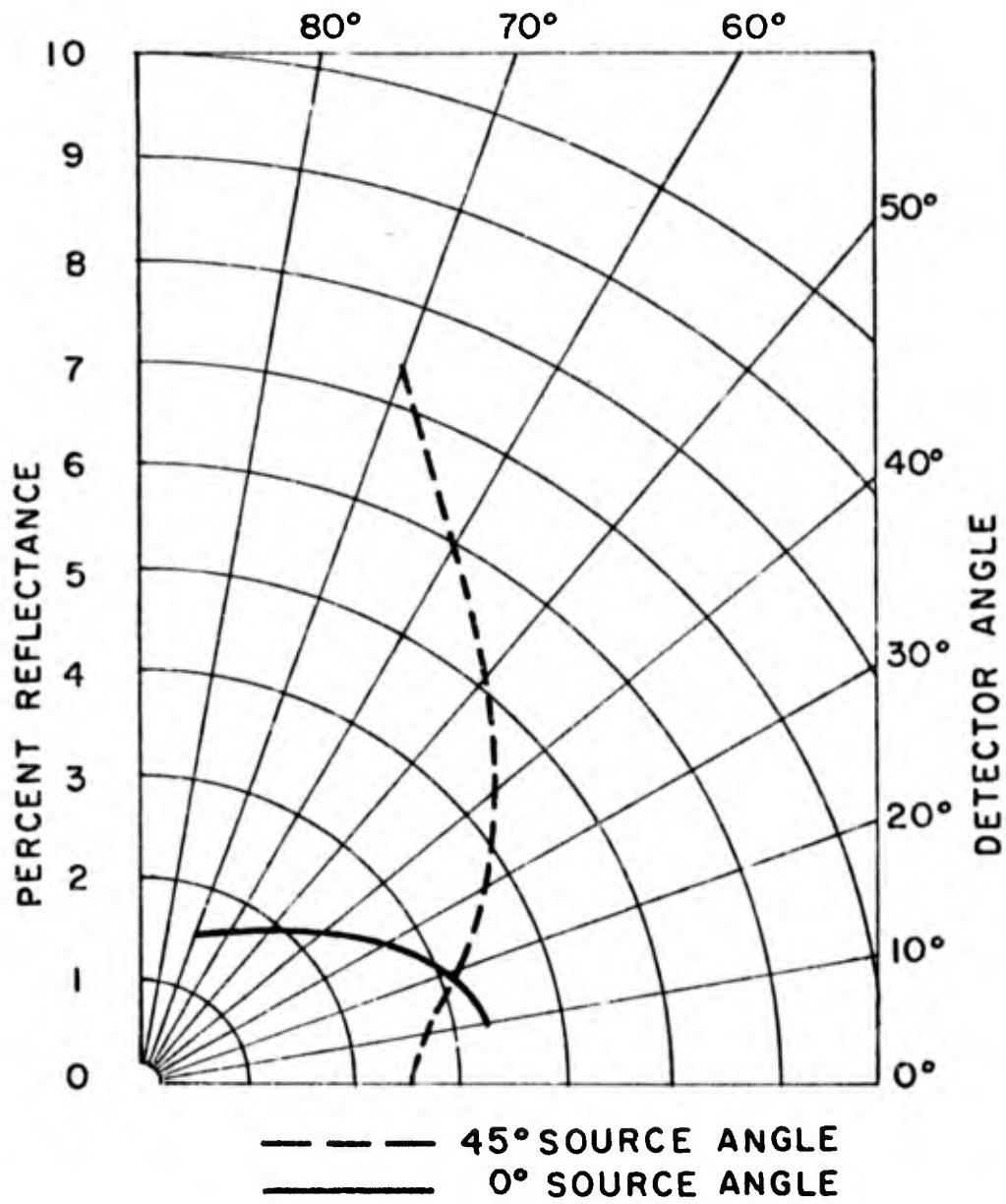


Figure 13. Percent Reflectance From Surface of High-Contrast Layer With Insulating Layer Behind The High-Contrast Layer

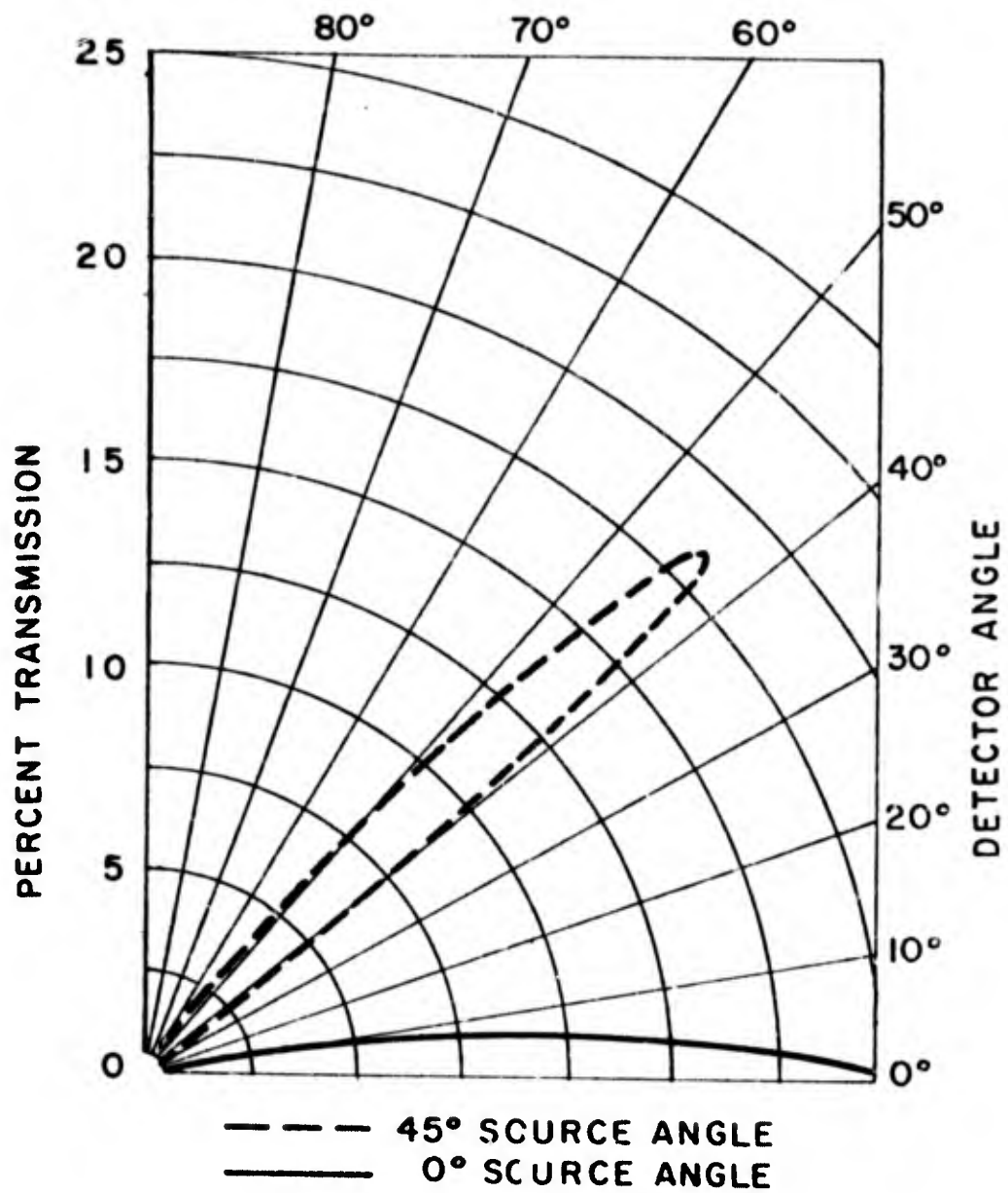


Figure 14. Percent Transmission vs Viewing Angle for EL Lamp With High-Contrast Layer

Some attempts were made to apply the classical single particle theory to these results, but multiple scattering introduces considerable error into the equations. The problem is much too complex to be considered in any great detail in this project.

Sample EL lamps were made using the contrast filter developed previously. The results obtained above in the analysis indicated that this contrast layer was quite satisfactory and very little improvement could be achieved by further analysis of particle size. Shown in Figure 15 are reflectance curves for a typical EL lamp with the contrast filter between the front electrode and the phosphor layer for light incident normal to the surface and 45° from the normal. Two facts are quite obvious when compared with the reflectance curves obtained for the contrast filter on the phosphor layer. These results were shown in Figures 12 and 13. First, the reflectance values are lower for the lamp due to a smaller difference in refractive indices between the glass-front electrode-contrast layer combination as compared to that between air and the contrast layer. Second, we do not see the increasing reflectance values with angle of view. This is due to the fact that light reflected from the contrast layer back through the glass window is scattered in all directions. When the reflected light is incident on the glass-front electrode interface at an angle greater than the critical angle, it is totally reflected back into the interior of the lamp where it is absorbed. This reduces considerably the amount of light reflected at large viewing angles.

The reflectance curve for light incident at 45° also shows a very high peak when the viewing angle is 45° . This obviously is due to front surface reflection, since no such peak was observed when light is reflected directly from the surface of the contrast filter. It was also observed in these lamps that the specular reflection from the front electrode gave an objectionable color to the display panel.

A series of EL high-contrast lamps, with contrast layers having different transmittance factors, were prepared. The reflectance curves for 20%, 30%, 40% and 50% transmitting filters are shown in Figures 16, 17, 18, and 19, respectively. The results point out the fact that the reflectance factor is predominantly dependent on the absorption coefficient of the contrast layer. Each of the samples in Figures 16 through 19 also utilized an internal anti-reflection coating. This coating virtually eliminated the specular reflection from the NESAs front electrode.

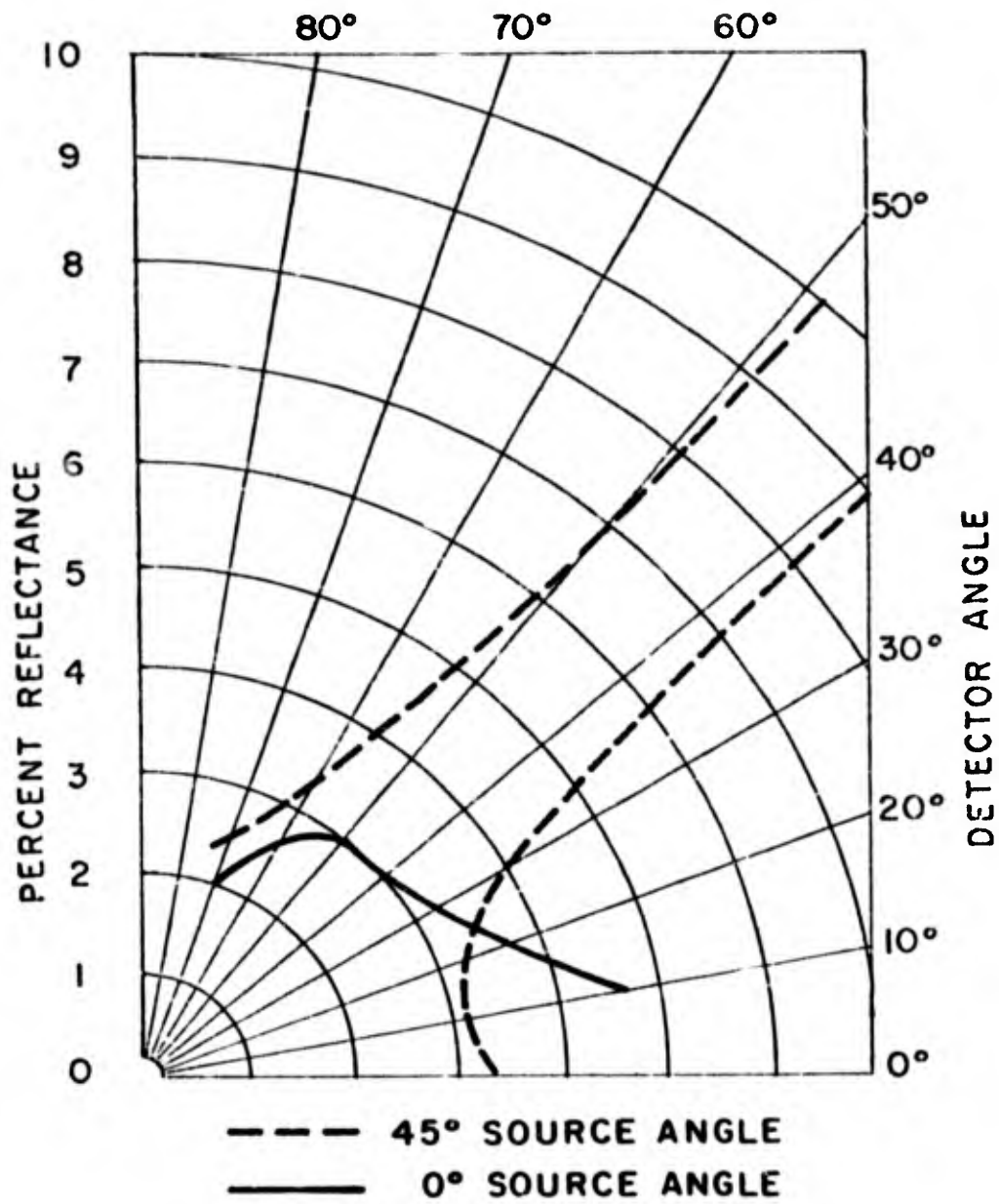


Figure 15. Percent Reflectance of EL Lamp With High-Contrast Layer

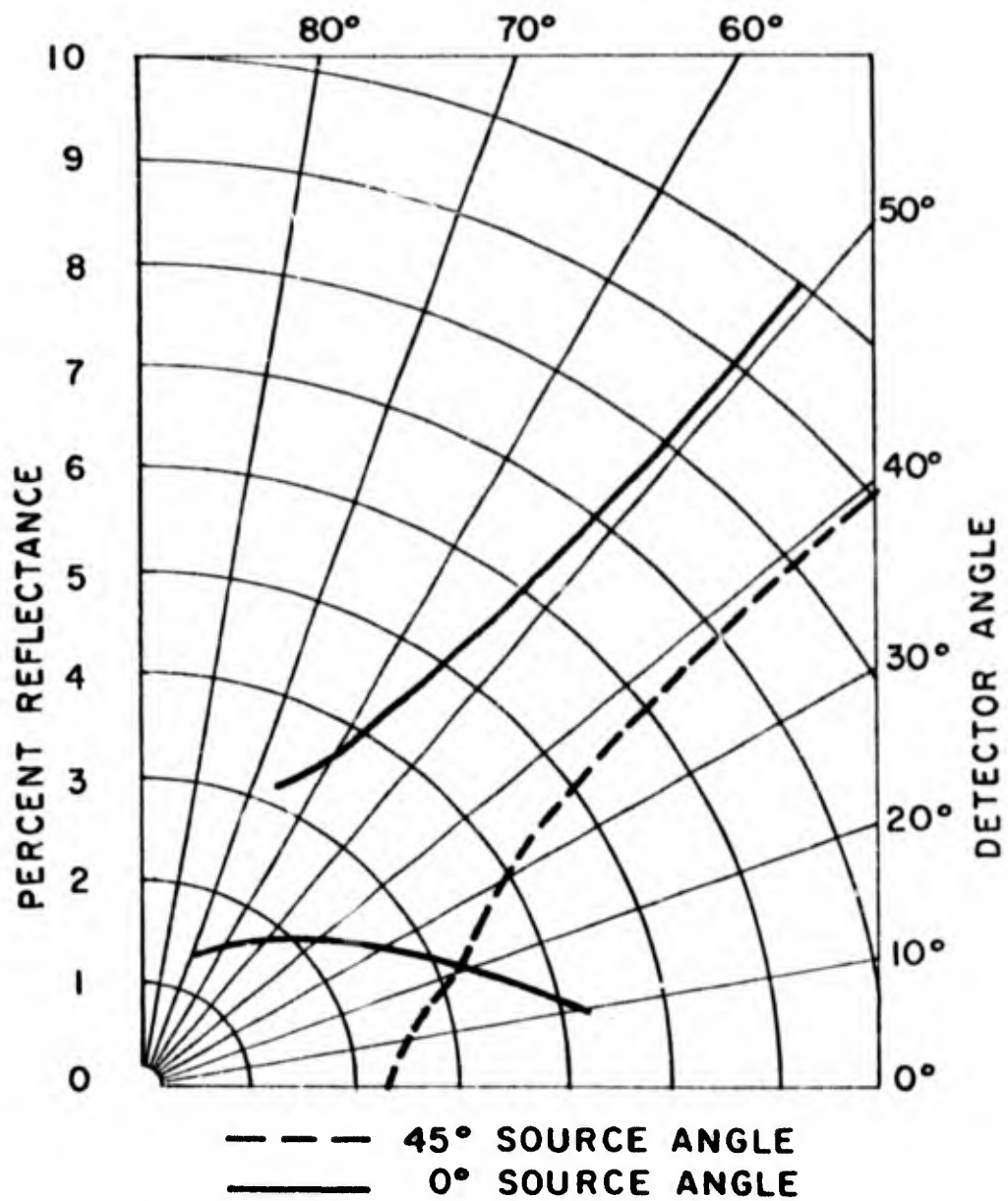


Figure 16. Percent Reflectance of EL Lamp With 20%-Transmitting High-Contrast Layer

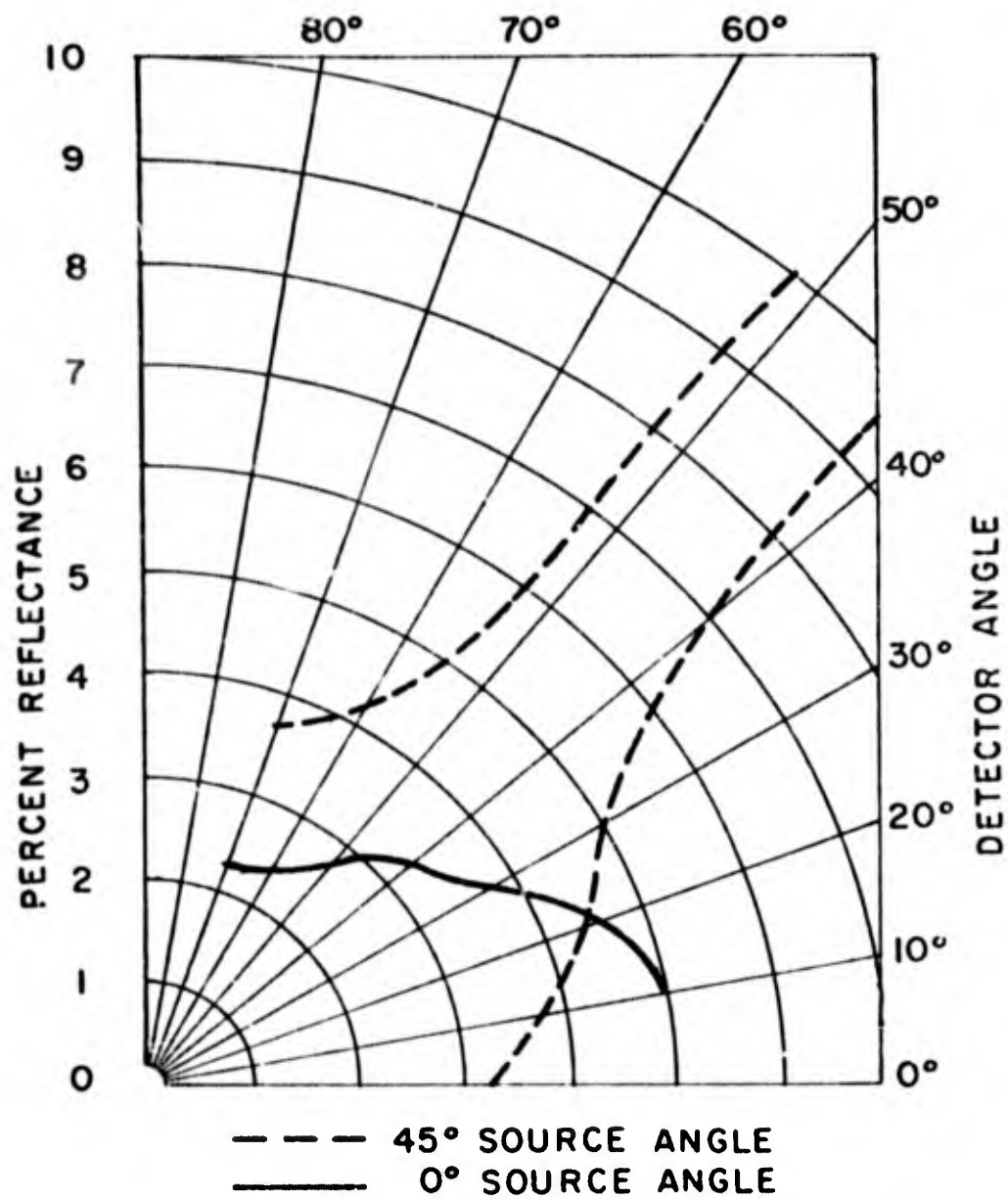


Figure 17. Percent Reflectance of EL Lamp With 30% Transmitting High-Contrast Layer

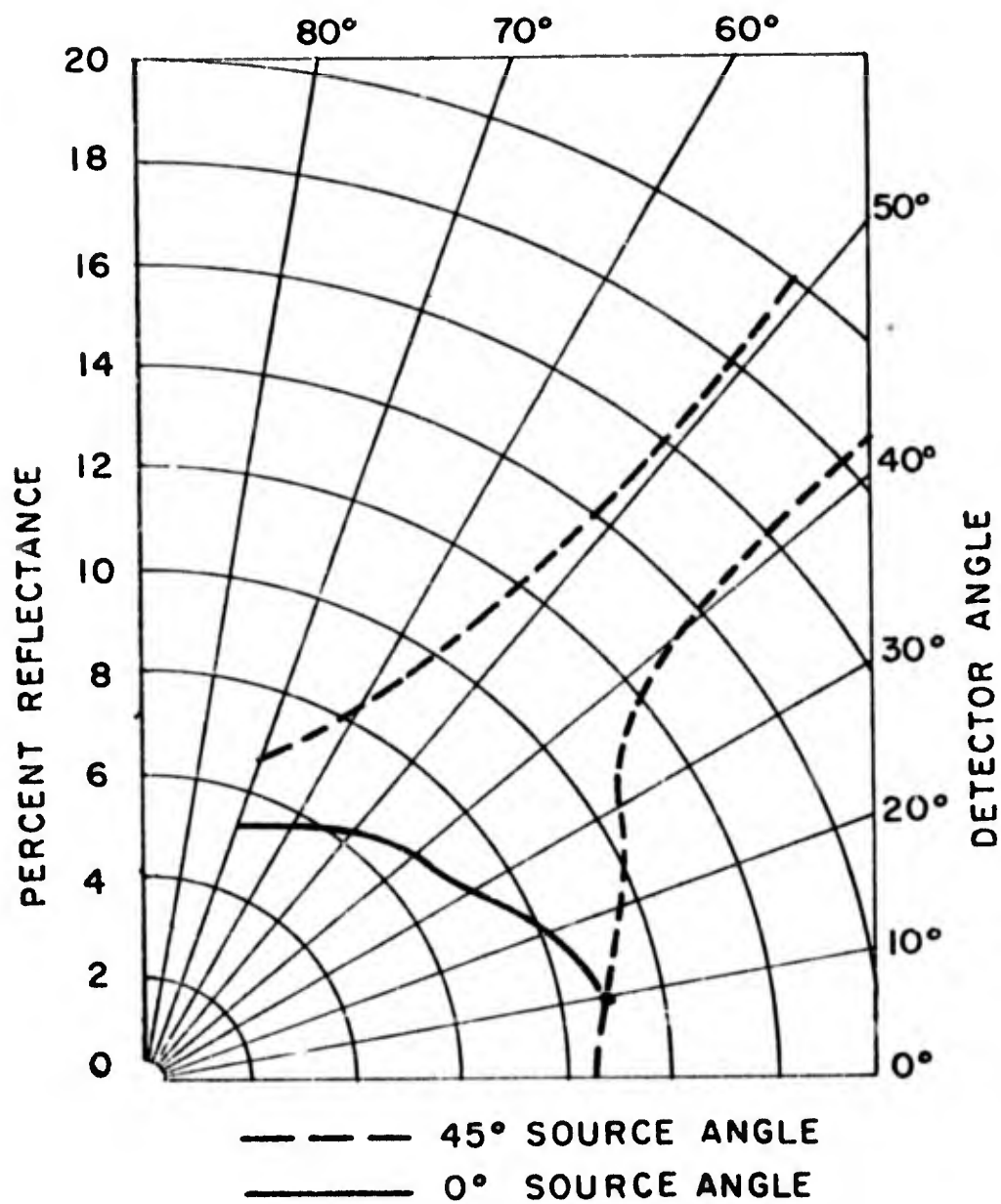


Figure 18. Percent Reflectance of EL Lamp With 40% Transmitting High-Contrast Layer

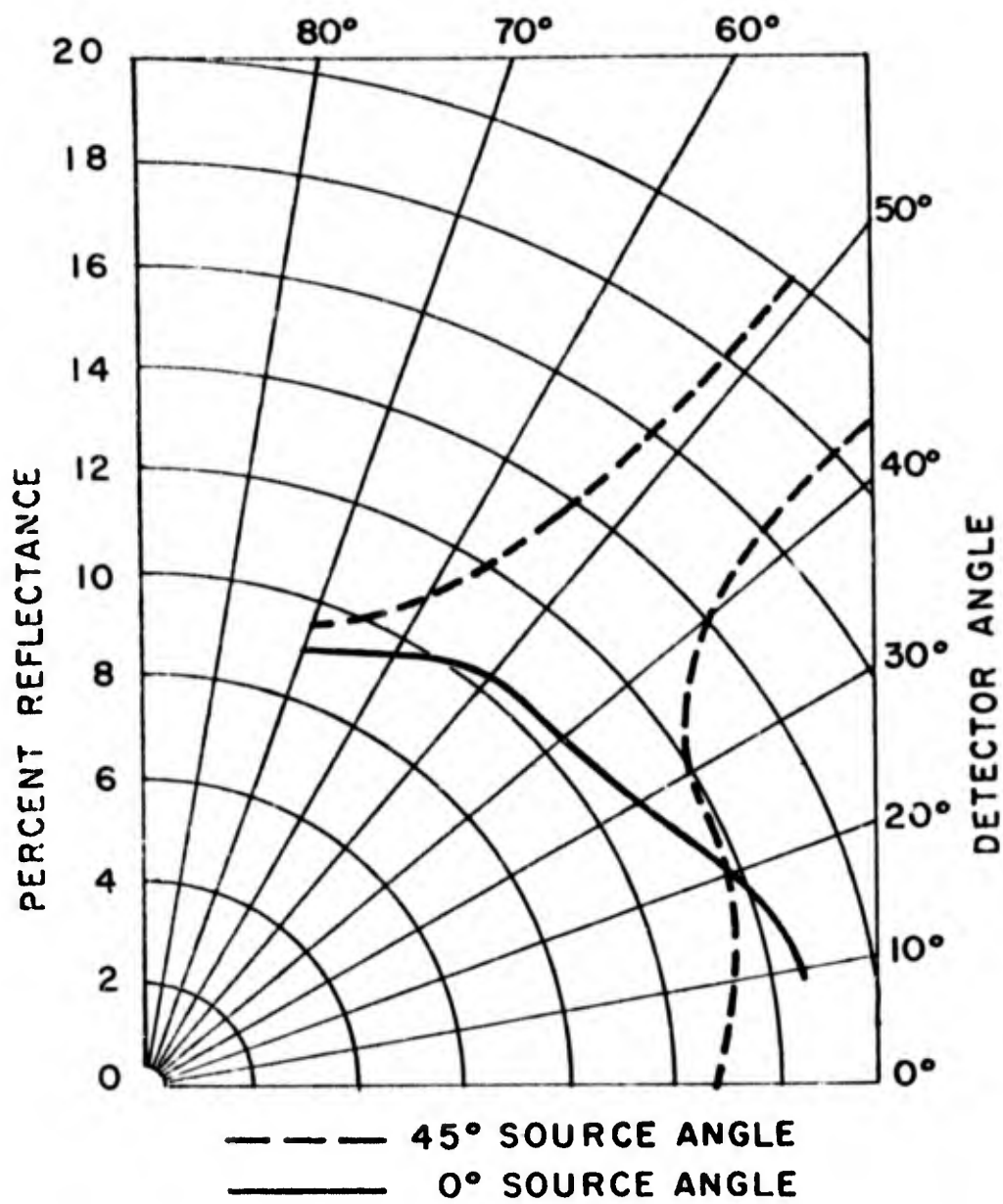


Figure 19. Percent Reflectance of EL Lamp With 50%-Transmitting High-Contrast Layer

Since there are other possible locations for the contrast filter in the EL panel, it was decided to run a series of tests to investigate this problem. Accordingly, test lamps were built composed of five different geometries. The first section had the contrast layer between the front electrode and the phosphor layer. The second section had a contrast layer between the phosphor layer and rear dielectric layer. The contrast layer was put between the dielectric layer and back electrode in the third section. The fourth section was a conventional EL lamp with no contrast layer. The contrast layer was deposited on the front surface of the fifth lamp. Brightness readings were taken on all five lamps. Reflectance measurements were also made. Figure 20 shows a plot of brightness vs. voltage for all five lamps. Table III gives the contrast ratios for these lamps at 250 volts, 400 cps.

Table III. Contrast Ratios for Various Positions of High-Contrast Layer in An EL Lamp

<u>Lamp No.</u>	<u>Contrast Ratio</u>
1	7.6
2	1.7
3	1.9
4	2.0
5	3.9

It is quite obvious from these results that the best position for the contrast filter is between the front electrode and the phosphor layer. The contrast ratio has a maximum value when this geometry is used.

The results of this investigation were also useful for analyzing the loss in brightness in the high contrast lamp. The loss in brightness is due to two mechanisms. There is an optical loss due to the absorption of the contrast layer and an electrical loss due to a capacitive voltage division caused by the insertion of the contrast filter between the electrodes of the EL configuration. The optical loss of a normal high contrast display is about 70%. The electrical loss is slightly over 10%.

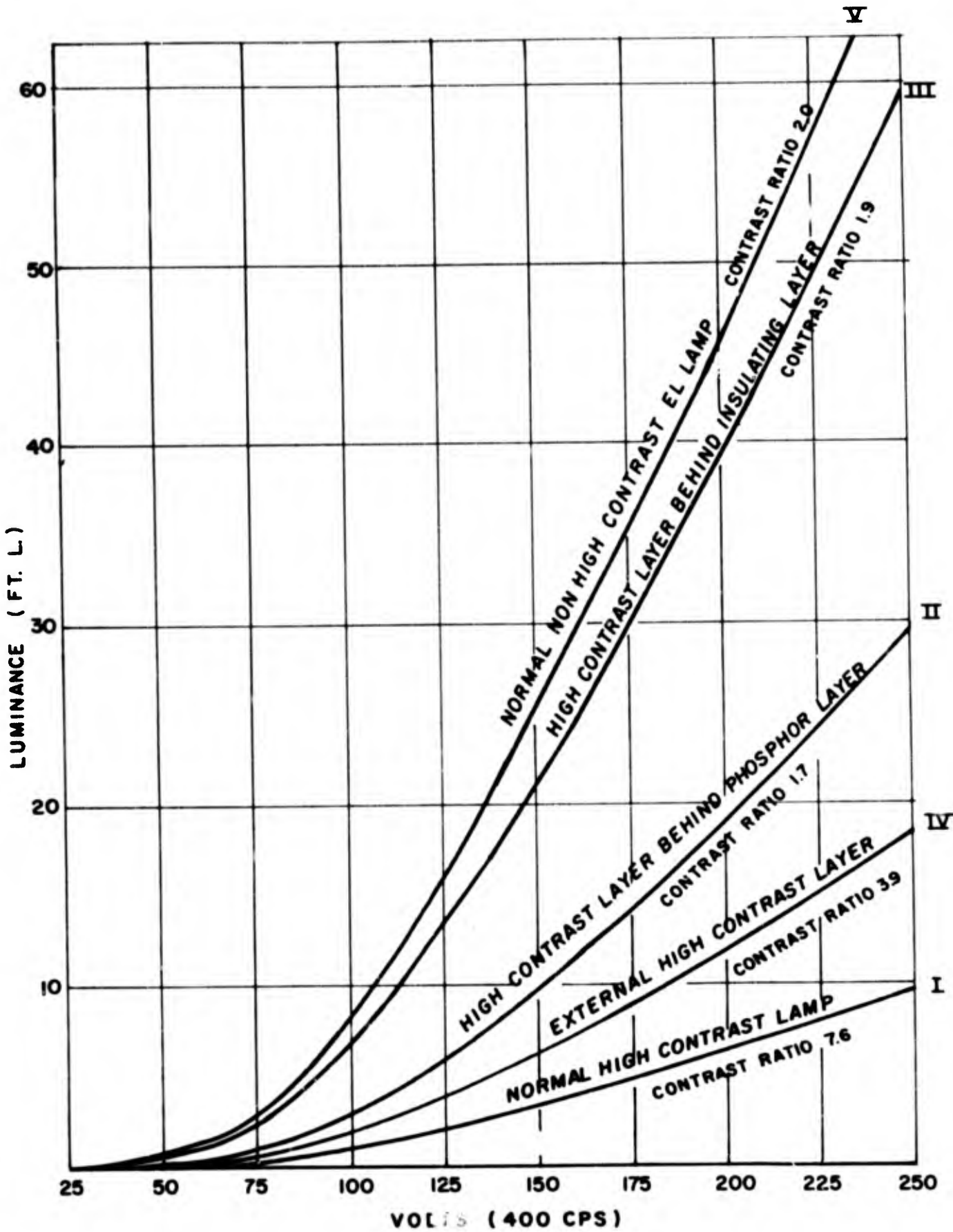


Figure 20. Luminance vs. Voltage High Contrast Layer Position Variable

A sample EL panel was fabricated using a gray glass substrate which has a transmittance of 31%. The reflectance curves are plotted in Figure 21. The reflectance factors are slightly higher than those obtained for a normal high contrast lamp. The transmittance factor was also investigated. The transmittance of the gray glass is a maximum in the direction of incident light and very little scattering is observed as compared to the contrast layer. Essentially, the gray glass is a solid colloidal system, i. e. , a glass matrix containing very small absorbing particles with diameters probably less than .05 micron. In this range of particle size, the primary extinction mechanism occurring is absorption and the scattering coefficient is very low.

Although the measured parameters would appear to indicate that the high contrast layer EL panel and the gray glass EL panel are similar, other considerations make them different. The color difference between the high contrast filter and the EL segment is much greater than that between the gray glass and EL segment, when filters of equal transmittance are compared. Also the high-contrast filter with its dispersion of opaque particles has a diffusion power and hiding power greater than exhibited by gray glass.

c. Anti-reflection Coating Measurements

As can be seen from the reflectance curves, the front surface reflection is very high when the angle of view equals the angle of incidence. Much of this directional reflectance is due to reflections from the glass substrate front surface and the glass-NESA interface. It was pointed out earlier that this problem can be alleviated by using some type of anti-reflection coating on these surfaces.

Samples were prepared using commercially available anti-reflection techniques. Three types were used, (1) "HEA", (Figure 22), (2) "Trucite", (Figure 23), and (3) "Velvetone", (Figure 24). HEA is a trade name for an anti-reflection coating composed of three vacuum deposited optical films. This combination is chosen to give less than 1/4% reflectance. The Trucite coating is just an etched glass surface to form a diffusing layer. The Velvetone coating also is a diffusing surface.

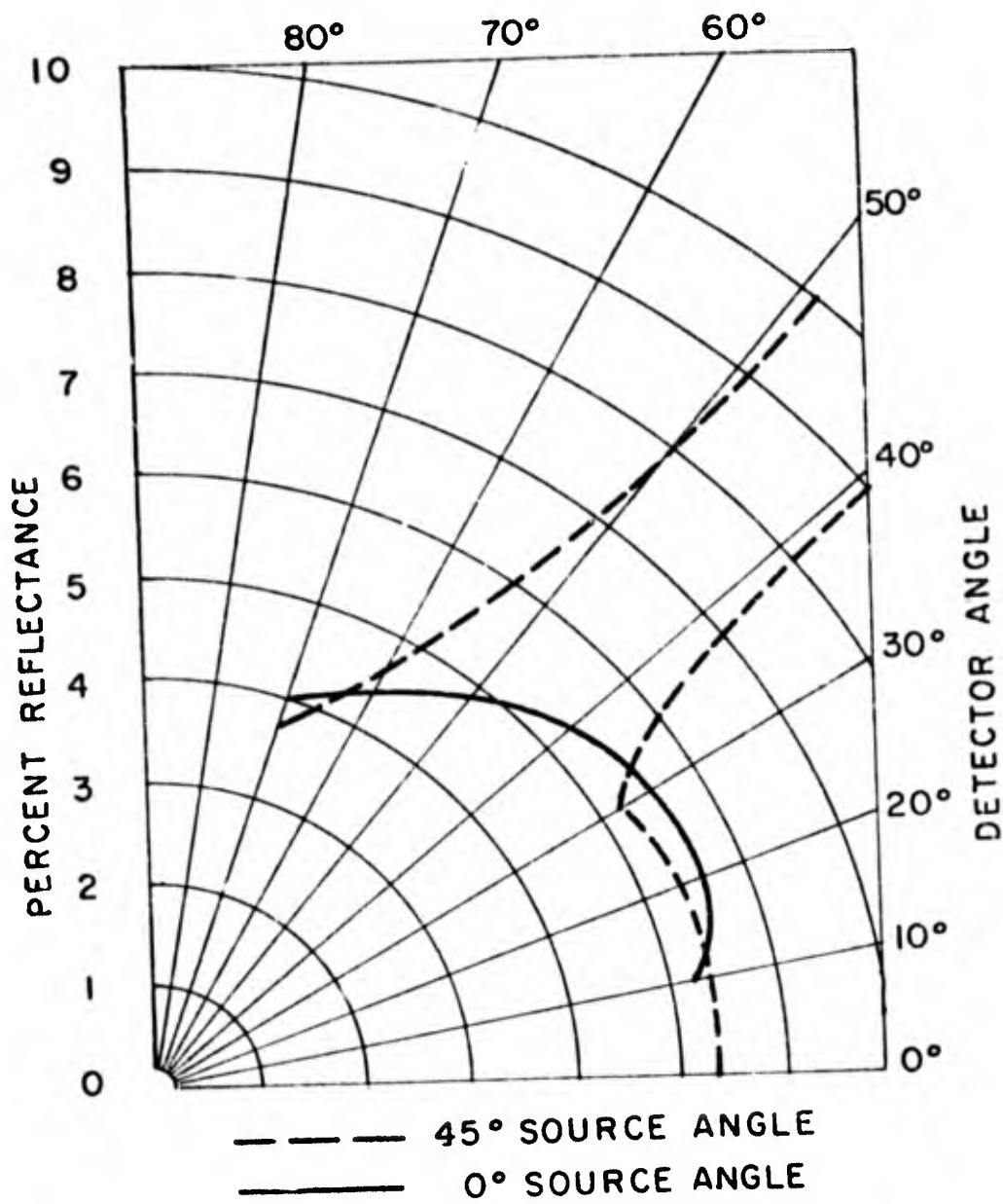


Figure 21. Percent Reflectance of EL Lamp With 30%-Transmitting Gray Glass Substrate

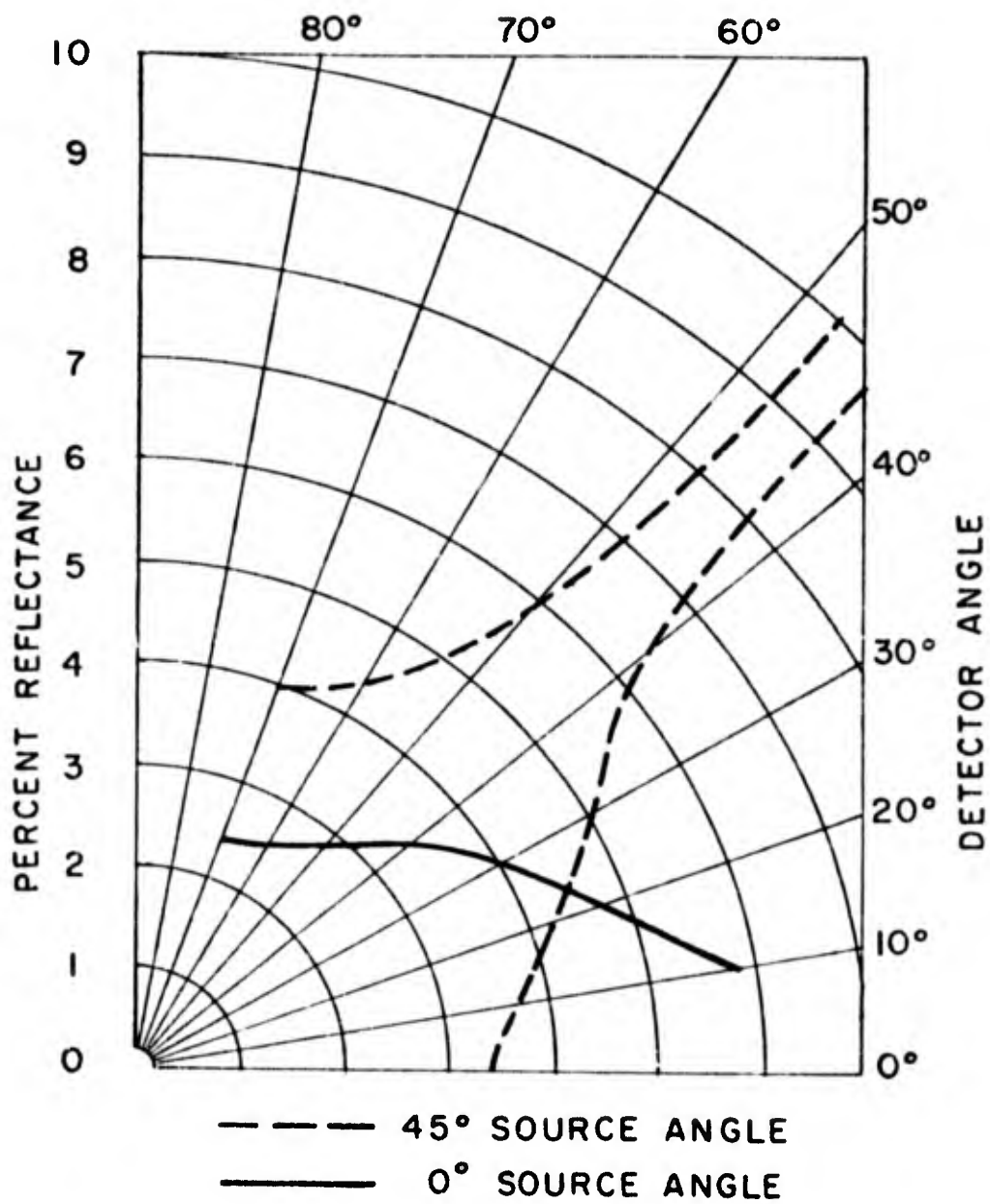


Figure 22. Percent Reflectance of High Contrast EL Lamp With HEA Coating on Front Surface

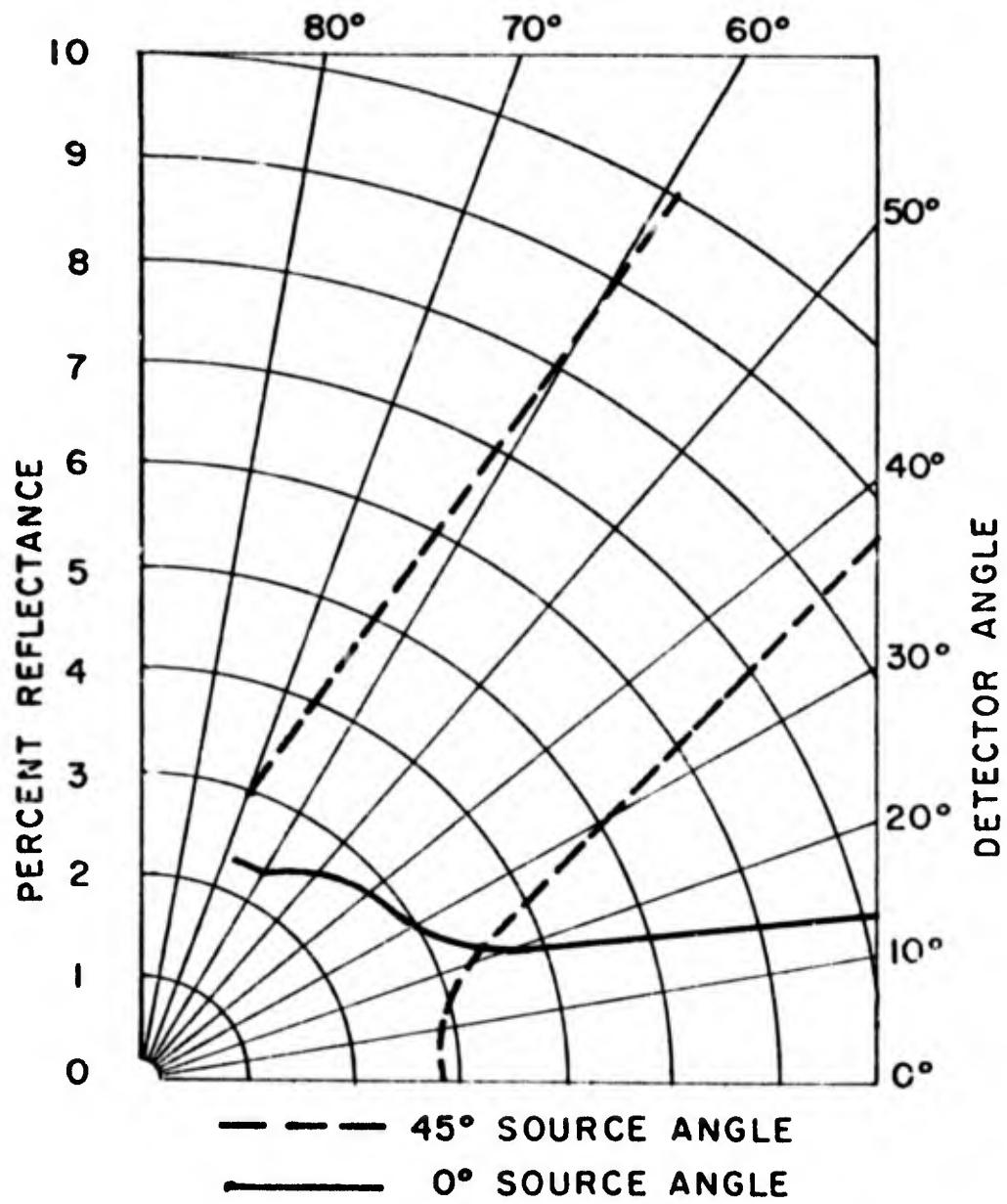


Figure 23. Percent Reflectance of High Contrast EL Lamp With Trucite Coating on Front Surface

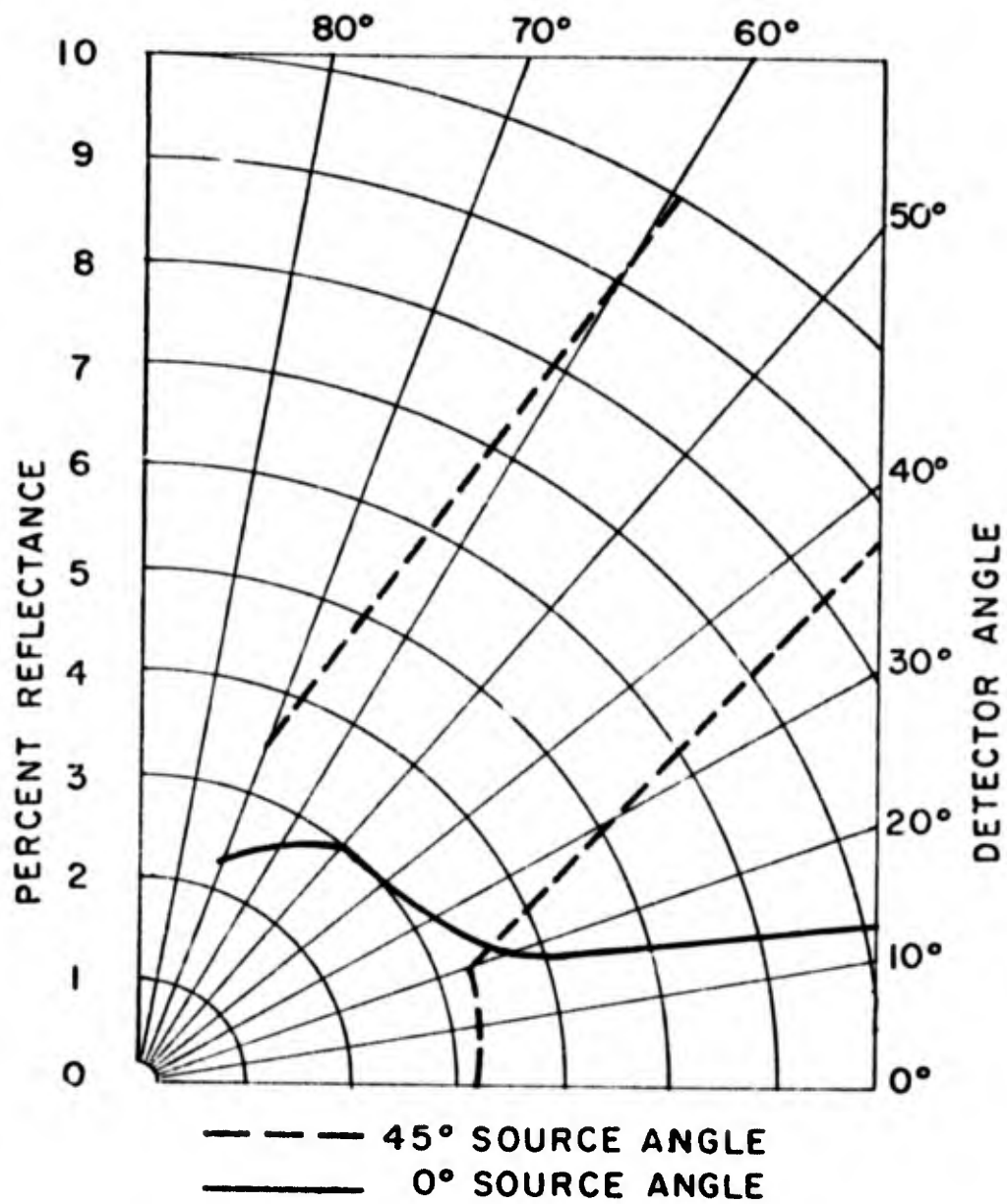


Figure 24. Percent Reflectance of High Contrast EL Lamp With Velvetone Coating on Front Surface

Figures 22, 23, and 24 show reflectance curves for EL displays with these three anti-reflection coatings.

The sample with the HEA coating also has an internal coating which removes the specular reflection from the NESA-glass interface. All three samples used 30% transmission contrast filtering. Both the HEA and Trucite coatings have reduced the directional reflectance considerably, however, the Trucite coating has a very high backscatter coefficient and a high reflectance factor over a wide range of viewing angle. The Corning Velvetone has done very little in reducing the directional reflectance and also has a high backscatter coefficient similar to the Trucite. Obviously, both the Trucite and Velvetone coatings are good scattering media but they do introduce increased reflectance in the back direction. As a result, the HEA coating has been chosen for use in EL displays fabricated for this project.

The application of the HEA coating underscores the problem of iridescent specular reflection from the glass transparent electrode interface. A special coating must be used to eliminate the specular reflectance of this interface when applied over the transparent front electrode surface. This addition does not appear to change other optical and electrical parameters of the EL configuration to any great extent.

Figure 25 depicts reflectance curves for a completed landing sequence display. The lamp has a 27% transmitting contrast filter with a coating to eliminate the objectionable specular reflectance of the front electrode, and an HEA anti-reflection coating to eliminate the specular reflectance of the glass surface.

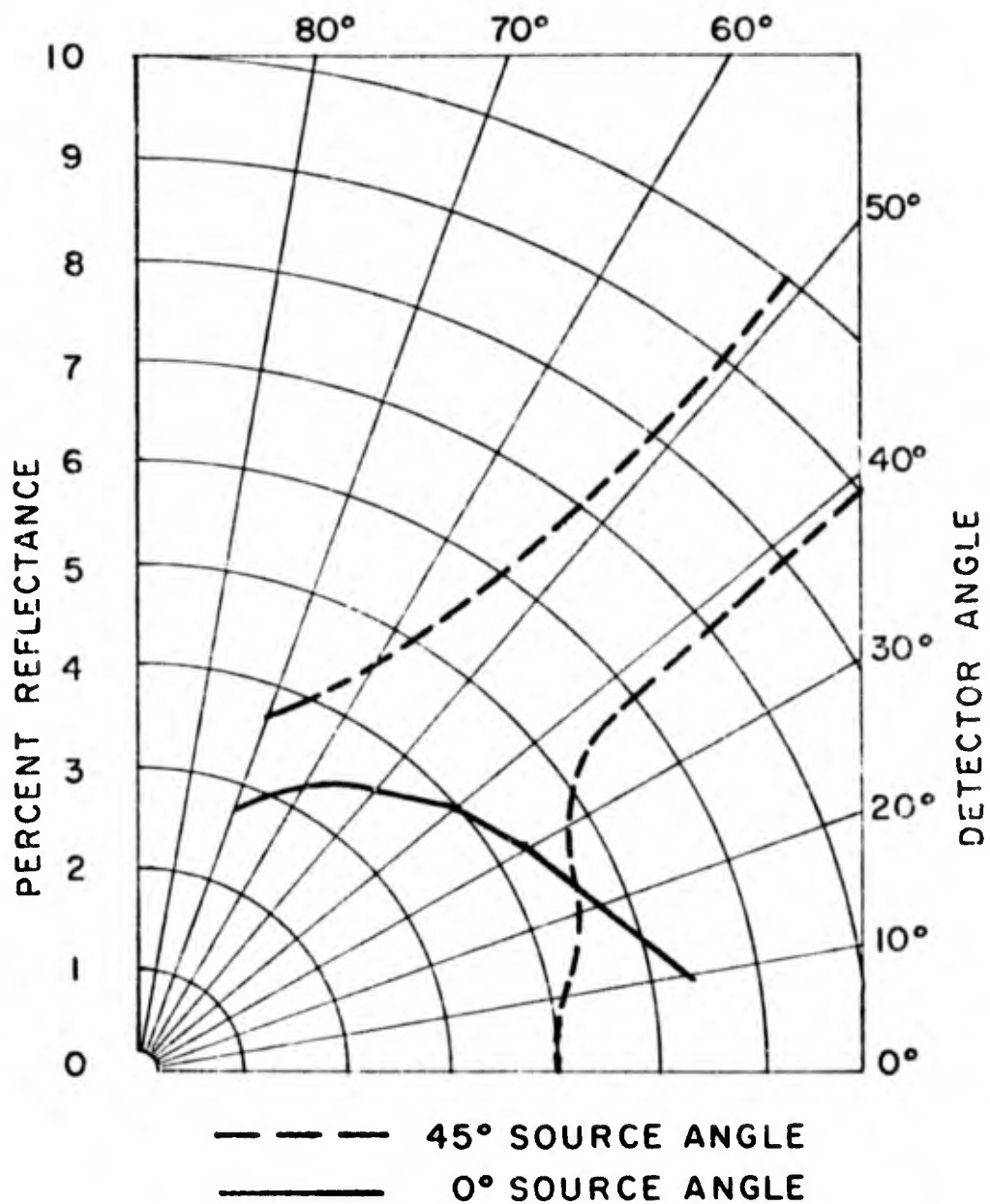


Figure 25. Percent Reflectance of EL Landing Sequence Lamp

SECTION IV

HUMAN FACTORS STUDY

1. METHODS AND RESULTS

The basic problem of the human factors study was to determine the visibility and legibility of EL numeric displays under a wide range of environmental illumination.

Test apparatus consisted of a fixed base part-task simulator, Figure 26, which is referred to as the Terradyne. Both subject and experimenter sat in the Terradyne such that the subject could not observe the experimenter's control actions, but the experimenter could observe and verify the subject's responses.

The subject sat facing an 18-inch by 18-inch square glare screen located about 30 inches in front of and level with the subjects head. This glare screen consisted of twelve 20-inch daylight fluorescent tubes mounted with their sides touching, and it simulated an aircraft windscreen with a view of a cloud mass reflecting direct sunlight.

Directly below the glare screen was a black instrument panel, Figure 27, containing three EL numeric displays. The numeric displays consisted of a plus or minus sign and five seven-stroke digits. The five digits were selected by the experimenter from a table of random numbers and controlled manually by means of five rotary switches. The experimenter controlled the voltage and luminance of the long life displays, operated individually, with a variac, and he recorded voltages required for the thresholds of legibility and rapid readability. Later, in reducing his data, the experimenter referred to voltage-luminance curves that had been prepared for each display.

Located a few inches above and to either side of the subject's head were two 750-watt daylight photo flood lamps and reflectors that were aimed at the glare screen and the EL displays. When these were turned on, and the glare screen fluorescents were turned on, a "worst condition" was created representing direct sunlight coming over the subject's shoulders and illuminating a cloud bank in front of the windscreen. This condition was painful to the subject's eyes.

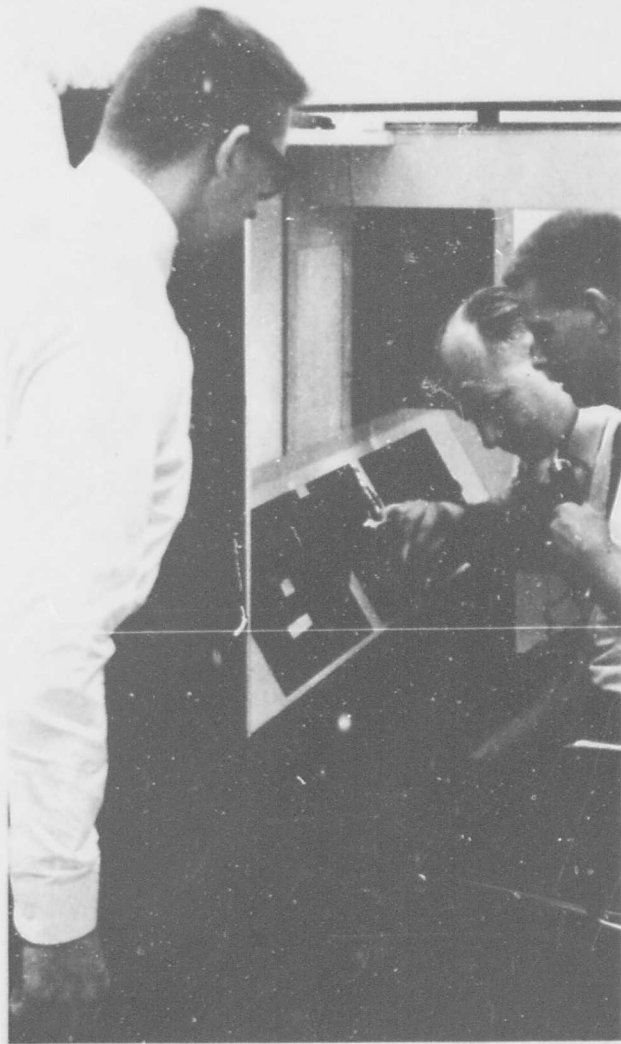


Figure 26. Terradyne Part-Task Simulator

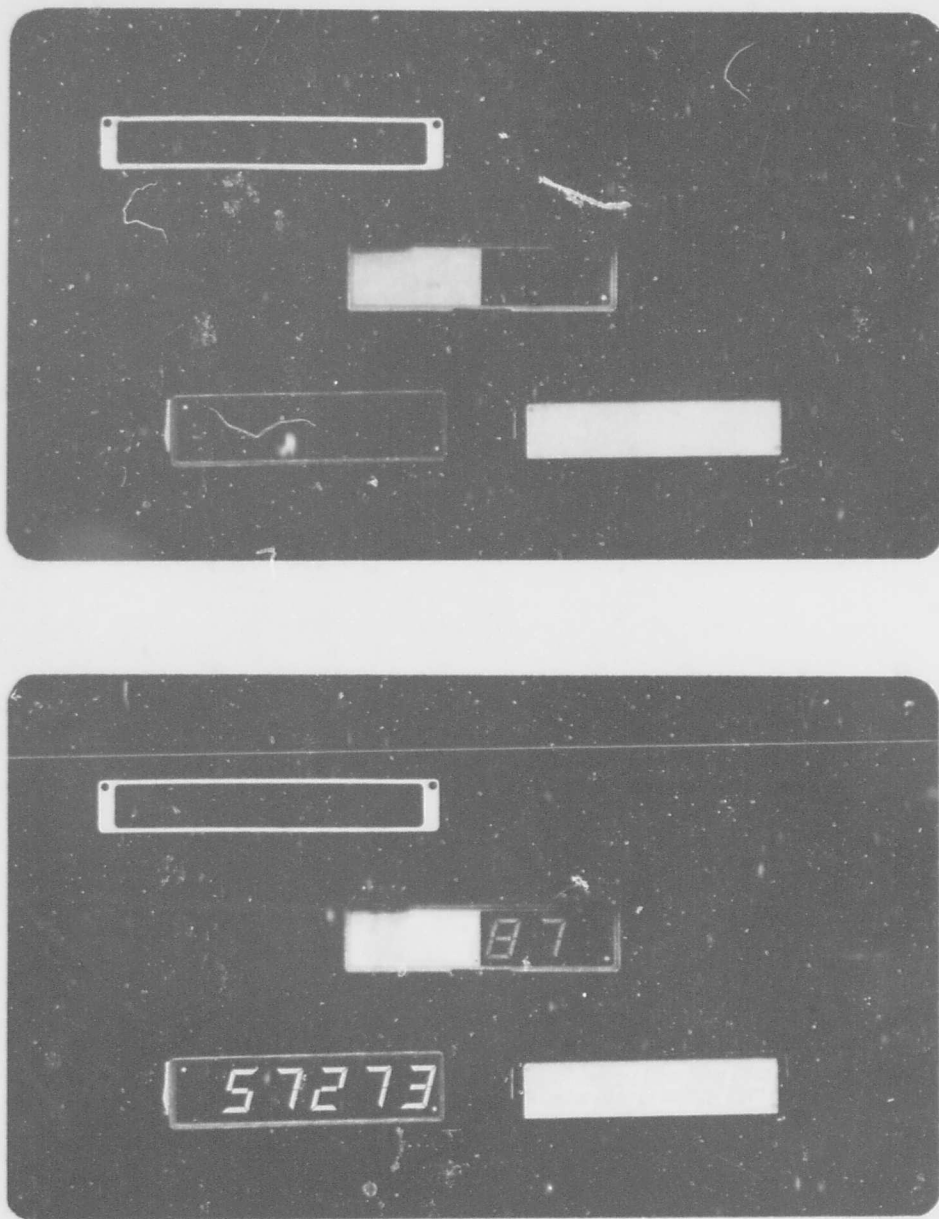


Figure 27. Regular, High-Contrast, and Improved High Contrast Displays

Four experiments using 45 subjects yielded over 7000 measurements using this apparatus. Four illumination conditions were used during each experiment. Three basic EL display constructions were tested:

- a. Normal EL construction having a white appearance with approximately 47% diffuse reflectance and 6% specular reflectance at near-normal incidence.
- b. "Original" high contrast EL construction having a 30% transmitting filter giving about 4-1/2% diffuse reflectance and 6% specular reflectance at near-normal incidence.
- c. "Improved" high contrast EL construction having a 30% transmitting filter giving about 5% diffuse reflectance and with external and internal anti-reflection coatings giving about 1/2% specular reflection.

The four conditions of illumination used in the last two experiments are shown in Table IV.

Table V is a summary of the median threshold of numeric luminance required for rapid and accurate reading as determined in the last two experiments, representing 30 subjects and 3000 data points. These luminance values represent total luminance minus the reflected luminance, yielding EL emission luminance only.

Table VI is the same as Table V except that luminance values have been converted to actual contrast ratios, based on luminance factors measured in the test apparatus using a magnesium oxide reflectance standard. Luminance measurements were made using a Spectra Pritchard Model 1973 PR Spot Photometer having a corrected photopic response.

In Table VI the reason that the "Original" high-contrast numeric requires consistently higher contrast ratios for rapid readability, than even the normal EL numeric, is that specular reflections from the subject and apparatus represent a larger fraction of the total display reflectance in the former case. The effectiveness of the anti-reflection coatings in improving performance is clearly shown.

Table IV. The Four Conditions of Illumination Used for the Human Factors Study

	<u>Intensity at Windscreen in Ft. - Lamberts</u>	<u>Intensity at Subject's Eyes in Ft. - Candles</u>	<u>Intensity at Display Panel in Ft. - Lamberts</u>
<u>Condition I</u>			
2 photofloods Windscreen (12 fluorescents) Lab ceiling Luminaire Terradyne fluorescents	5,000 to 5,300	650	1350-Magnesium Oxide standard
<u>Condition II</u>			
Same as Condition I minus the 2 photofloods	2,000 to 3,700	260	105-Magnesium Oxide
<u>Condition III</u>			
Same as Condition II minus the windscreen fluorescents	12 to 20 Hot spot 49	38	49-Magnesium Oxide
<u>Condition IV</u>			
Same as Condition III minus lab. Luminaire	4 to 22 Hot spot 49	5.2	18-Magnesium Oxide

Table V. Summary of Median Threshold of Numeric Luminance Required for Rapid and Accurate Reading

	<u>Improved High Contrast EL</u>	<u>High Contrast EL</u>	<u>Conventional (Clear) EL</u>
Condition I	1.31 Ft. L.	9.6 Ft. L.	36.0 Ft. L.
Condition II	.12 Ft. L.	1.7 Ft. L.	6.5 Ft. L.
Condition III	.05 Ft. L.	.12 Ft. L.	1.2 Ft. L.
Condition IV	.015 Ft. L.	.05 Ft. L.	.3 Ft. L.

Table VI. Luminance Values From Table V Converted Into Contrast Ratios

	<u>Improved High Contrast EL</u>	<u>High Contrast EL</u>	<u>Conventional (Clear) EL</u>
Condition I	0.018	0.16	0.056
Condition II	0.019	0.33	0.12
Condition III	0.019	0.057	0.055
Condition IV	0.010	0.056	0.032

2 CONCLUSIONS

The results of the human factors experiments are exceptionally clean-cut. The differences observed among the different type displays are of both practical and statistical significance. The original high contrast display is superior to the conventional clear display, particularly at high incident illumination levels, and the improved high-contrast display is -- in turn -- significantly superior to both the original high contrast and clear conventional displays.

Since, at normal operating voltages, the improved high-contrast display will emit 10 to 20 times the luminance required for rapid reading under the worst condition tested (condition 1), there is every reason to be confident that an EL display utilizing this construction will be seen clearly and read accurately in an aircraft cockpit during all daylight lighting conditions.

APPENDIX

EXTINCTION AND DISPERSION IN A MEDIUM CONTAINING PARTICLES

When light passes through the surface of a layer containing dispersed particles, it enters a region containing small particles or clusters of particles with optical properties more or less different from those of the vehicle; this region is, not homogeneous to a bundle of light energy. Once within the confines of the layer, the light must either re-emerge or be dissipated as some other form of energy, since energy cannot be destroyed. The conversion of light energy into some other form is known as absorption. It may occur either in the medium containing the particles or in the particles themselves.

The other mechanism by which light may be affected within the layer is scattering, a sort of reflection occurring at the interface between the medium in which the light is traveling and a particle of different refractive index. Scattering is fundamentally an interaction of electromagnetic radiation with a particle to produce a redirection of energy. If the particle is large compared with the wavelength of incident radiation, reflected and refracted energy can be distinguished from diffracted energy; but for small particles, no such distinction is possible.

Both scattering and absorption remove energy from a beam of light traversing the medium, i.e., the beam is attenuated. This attenuation is called extinction. Thus defined we can write

$$\text{Extinction} = \text{Scattering} + \text{absorption}$$

The scattering of electromagnetic radiation by a particle is discussed in many texts 1, 2, 3, 4. Scattering processes are traditionally described by the differential cross-section which is defined as the time-averaged outgoing flux per unit time per unit solid angle divided by the time-averaged incident flux. For the case of electromagnetic radiation (light) the flux is described by Poynting's theorem.

The differential cross-section may be integrated over a solid angle to yield the total cross-section. Thus the total cross-section may be expressed in terms of an absorption cross-section, σ_{abs} , the scattering cross-section, σ_{scat} ; and the incident energy. If the total

extinction cross-section σ_{ext} , is set equal to the total energy removed from the incident beam, the conservation of energy requires that

$$\sigma_{\text{ext}} = \sigma_{\text{sca}} + \sigma_{\text{abs}}$$

The basic Mie equations for the extinction, scattering, and absorption cross-sections of particle systems are:

$$\sigma_{\text{ext}} = \frac{2\pi r^2}{x^2} \sum_{n=1}^{\infty} (2n+1) \operatorname{Re}(a_n + b_n) \quad (1)$$

$$\sigma_{\text{sca}} = \frac{2\pi r^2}{x^2} \sum_{n=1}^{\infty} (2n+1) (|a_n|^2 + |b_n|^2) \quad (2)$$

and

$$\sigma_{\text{abs}} = \sigma_{\text{ext}} - \sigma_{\text{sca}} \quad (3)$$

where

r = radius of particle

$x = \frac{2\pi r}{\lambda_m}$ = size parameter

a_n, b_n = Mie coefficients

Re = real part of complex number

λ_m = wavelength of incident light in medium

The Mie coefficients are analytically represented by:

$$a_n = - \frac{j(Nx) [xj_n(x)]' - j_n(x) [Nxj_n(Nx)]'}{j_n(Nx) [xh_n^2(x)]' - h_n^2(x) [Nxj_n(Nx)]'} \quad (4)$$

$$b_n = - \frac{j_n(x) [Nxj_n(Nx)]' - N^2 j_n(Nx) [xj_n(x)]'}{h_n^2(x) [Nxj_n(Nx)]' - N^2 j_n(Nx) [xh_n^2(x)]'} \quad (5)$$

where N is the refractive index of the particle, η_1 , relative to that of the medium, η_2 .

$j_n ()$ = a spherical Bessel function

$h_n^2 ()$ = a spherical H \ddot{a} nk \ddot{a} l function of the second kind

The primes on the brackets denote differentiation with respect to the argument of the Bessel function within the bracket:

$$[xj_n(x)]' = \frac{d}{dx} [xj_n(x)]$$

We can also derive a backscattering cross-section:

$$\sigma_{bsco} = \frac{2\pi r^2}{X^2} \left| \sum_{n=1}^{\infty} (2n+1) (-1)^n (a_n - b_n) \right|^2 \quad (6)$$

In Mie theory, calculations are made for efficiency factors which are cross-sections divided by the geometric cross-section of the scattering particle. The expressions obtained are:

$$\text{Extinction Efficiency} = Q_{ext} = \frac{\sigma_{ext}}{\pi r^2} \quad (7)$$

$$\text{Scattering Efficiency} = Q_{\text{sca}} = \frac{\sigma_{\text{sca}}}{\pi r^2} \quad (8)$$

$$\text{Backscattering Efficiency} = Q_{\text{bsca}} = \frac{\sigma_{\text{bsca}}}{\pi r^2} \quad (9)$$

and

$$Q_{\text{ext}} = Q_{\text{obs}} + Q_{\text{sca}} \quad (10)$$

We are also interested in the amplitude and intensity of the scattered light as a function of the scattering angle. From Mie's theory the equations for the amplitude function are:

$$S_1(N, X, \theta) = \sum_{n=1}^{\infty} \frac{2n+1}{n(n+1)} \left\{ a_n \pi_n + b_n \tau_n \right\} \quad (11)$$

$$S_2(N, X, \theta) = \sum_{n=1}^{\infty} \frac{2n+1}{n(n+1)} \left\{ b_n \pi_n + a_n \tau_n \right\} \quad (12)$$

where S_1 and S_2 are the dimensionless, complex amplitude functions related to the components polarized in the planes perpendicular and parallel, respectively, to the scattering plane. The quantities π_n and τ_n are functions of the scattering angle and are known as associated Legendre polynomials.

If we take the squares of the complex amplitudes we have

$$i_1(N, x, \theta) = \left| S_1 \right|^2, \quad i_2(N, x, \theta) = \left| S_2 \right|^2 \quad (13)$$

For incident unpolarized light, I_0 , the intensity of scattered light, I , is

$$I = \frac{\frac{1}{2} (i_1 + i_2)}{\omega^2 R^2} \quad (14)$$

where ω is the wave number, $\omega = \frac{2\pi}{\lambda}$ and R is the distance from the particle.

It must be emphasized that the discussion above applies only to particle systems in which the concentration of particles is low. This would allow each individual particle to formulate its own reflection and refraction wave pattern. As soon as the particle concentration is such that the wave front developed by each particle interferes with the wave fronts from neighboring particles, multiple scattering takes place and it is no longer possible to use the above equations to calculate extinction, scattering and absorption coefficients for the particular system.

REFERENCES

1. Born, M. and Wolf, E., Principles of Optics, Pergamon Press, New York (1959).
2. Jackson, J. E., Classical Electrodynamics, John Wiley and Sons, Inc., New York (1962).
3. Landau, L. D. and Lifshitz, E. M., The Classical Theory of Field, Addison-Wesley Publishing Co., Inc., Reading, Mass. (1962).
4. Van de Hulst, H. C., Light Scattering by Small Particles, John Wiley and Sons, Inc., New York (1957).

BIBLIOGRAPHY

GENERAL

Peterson, Capt. C. J. and Smith, H. A., Development of High Contrast Electroluminescent Techniques for Aircraft Displays Presented to the Ninth Annual Human Factors Society Meeting - October 1965.

Petertyl, S. V. and Fuller, P. R., Improved Contrast and Visibility for Electroluminescent Displays. Presented to the 18th Annual National Aerospace Electronics Conference - May 1966.

TECHNIQUE DEVELOPMENT

Aden, A. L., "Electromagnetic Scattering from Spheres with Sizes Comparable to the Wavelength," Journal of Applied Physics, Vol. 22, No. 5, pp. 601-605, (May 1951).

Blevin, W. R. and Brown, W. J., "Effect on Particle Separation on the Reflectance of Semi-Infinite Diffusers," Journal of the Optical Society of America, Vol. 51, No. 2, pp. 129-134 (February 1961).

Brillouin, L., "The Scattering Cross Section of Spheres for Electromagnetic Waves, Journal of Applied Physics, Vol. 20, No. 11, pp. 1110-1125 (November 1949).

Clewell, D. H., "Scattering of Light by Pigment Particles," Journal of the Optical Society of America, Vol. 31, No. 8, pp. 521-527 (August 1941).

Deirmendjian, Detal, "Mie Scattering with Complex Index of Refraction," Journal of the Optical Society of America, Vol. 51, No. 6, pp. 620-633 (June 1961).

Giovanelli, R. G., "Radiative Transfer in Discontinuous Media," Australian Journal of Physics, Vol. 10, pp. 227-239 (1957).

Goldberg, B., "New Computation of the Mie Scattering Functions for Spherical Particles, Journal of the Optical Society of America, Vol. 43, No. 12, pp. 1221-1222 (December 1953).

Harding, R. H., An Investigation into the Optical Properties of Pigmented Films, Ph. D. Dissertation, Purdue University (January 1958).

Harding, R. H., Golding, Band Morgen, R. A., "Optics of Light - Scattering Films. Study of Effects of Pigment Size and Concentration," Journal of the Optical Society of America, Vol. 50, No. 5, pp. 446-455 (May 1960).

Johnson, J. C. and Terrell, J. R., "Transmission Cross Sections for Water Spheres Illuminated by Infrared Radiation," Journal of the Optical Society of America, Vol. 45, No. 6, pp. 451-454 (June 1955).

Judd, Deane B., "Fresnel Reflection of Diffusely Incident Light," Journal of Research N. B. S., Vol. 29, pp. 329-332 (November 1942).

Krascella, N. L., "Theoretical Investigation of the Absorption and Scattering Characteristics of Small Particles," NASA Contractor Report CR-210 (April 1965).

Kubelka, Paul, "New Contributions to the Optics of Intensely Light-Scattering Materials," Part I, Journal of the Optical Society of America, Vol. 38, No. 5, pp. 445-457 (May 1948).

Lanzo, C. D., and Ragsdale, R. G., "Experimental Determination of Spectral and Total Transmissivities of Clouds of Small Particles," NASA Technical Note D-1405 (September 1962).

Marteney, R. J., "Experimental Investigation of the Opacity of Small Particles; NASA Contractor Report CR-211.

Melamed, N. T., "Optical Properties of Powders." Part I. "Optical Absorption Coefficients and the Absolute Value of the Diffuse Reflectance." Part II. "Properties of Luminescent Powders," Journal of Applied Physics, Vol. 34, No. 3, pp. 560-570, (March 1963).

Pendorf, R., "Total Mie Scattering Coefficients for Spherical Particles of Refractive Index 2.00," Journal of the Optical Society of America, Vol. 46, No. 11, p. 1001 (November 1956).

Sinclair, David, "Light Scattering by Spherical Particles," Journal of the Optical Society of America, Vol 37, No. 6, pp. 475-480 (June 1947).

HUMAN FACTORS

Baker, C. A., Debons, A., and Morris, D. F. Dark adaptation as a function of the intensity and distribution of light across the preadaptation field. *J. opt. Soc. Amer.*, 1956, 45 (6), 401-404.

Baker, C. A. and Grether, W. F. Visual presentation of information, WADC-TR-54-160, Wright Air Development Center, Wright-Patterson Air Force Base, Ohio, 1954.

Baker, H. D. The instantaneous threshold and early dark adaptation. *J. opt. Soc. Amer.*, 1953, 43 (9), 798-803.

Baker, H. D. et al., Early dark adaptation to dim luminances. *J. opt. Soc. Amer.* 1959, 49 (11), 1064-1070.

Baker, H. D. Initial stages of dark and light adaptation. *J. opt. Soc. Amer.* 1963, 53, (1), 98-103.

Christensen, J. M. Some typical sky and earth brightnesses at altitudes 10,000 to 40,000 feet and their relationship to the eye adaptation problems of the radar operator. USAF Hdq., AMC Engng. Div. Memo. Rep., 1946, Serial No. TSEAA-694-11.

Curtis, J. L. Visual problems of high altitude flight.

Gallup, H. F., Hambacher, W. D., and Dolby, J. R. Investigations into the optimal characteristics of visual warning and caution systems: The attention-getting value of a steady light as a function of brightness with respect to rapidity and reliability. USN AMC Rep., 1956, No. 301.

Gerathewohl, S. J. Conspicuity of steady and flashing light signals: variation of contrast. *J. opt. Soc. Amer.*, 1953, 43 (7), 567-571.

Siegel, A. I. and Stirner, F. W. Caution and warning light indicators for naval aircraft: IV. Background variation, letter size, and the advantages of a master indicator with yellow cautionary signals in a red illuminated environment. USN AMC ACEL Rep., 1957, No. 347.

USAF Air Research and Development Command. Handbook of instructions for aircraft designers. (HIAD) (10th ed.). Author Manual, 1954, No. AFSCM 801.

Woodson, W. E., and Conover, D. W. Human engineering guide for equipment designers (2nd ed.). Los Angeles: Univer. of Calif. Press, 1964.

Wulfeck, J. W., Weisz A., and Raben, M. W. Vision in military aviation, WADC-TR-58-399, Wright Air Development Center, Wright-Patterson Air Force Base, Ohio, 1958.

UNCLASSIFIED

Security Classification

DOCUMENT CONTROL DATA - R&D		
<i>(Security classification of title, body of abstract and indexing annotation must be entered when the overall report is classified)</i>		
1. ORIGINATING ACTIVITY (Corporate author) Lear Siegler, Inc. Instrument Division 4141 Eastern Ave., S.E. Grand Rapids, Mich.		2a. REPORT SECURITY CLASSIFICATION UNCLASSIFIED
		2b. GROUP N/A
3. REPORT TITLE DEVELOPMENT OF HIGH-CONTRAST ELECTROLUMINESCENT DISPLAYS		
4. DESCRIPTIVE NOTES (Type of report and inclusive dates) Final Report May 1 '65 - December 1 '66		
5. AUTHOR(S) (Last name, first name, initial) Petertyl, Sidney V. Fuller, Paul R. Wysocki, Chester, A		
6. REPORT DATE March 1967	7a. TOTAL NO. OF PAGES 66	7b. NO. OF REFS 5
8a. CONTRACT OR GRANT NO. AF 33(615)-2841	9a. ORIGINATOR'S REPORT NUMBER(S) Lear Siegler Publication No. GRR-67-1268	
b. PROJECT NO. 6190	9b. OTHER REPORT NO(S) (Any other numbers that may be assigned this report) AFDL-TR-66-183	
c. Task: 619009		
d.		
10. AVAILABILITY/LIMITATION NOTICES Distribution of this document is unlimited.		
11. SUPPLEMENTARY NOTES	12. SPONSORING MILITARY ACTIVITY Air Force Flight Dynamics Laboratory Wright Patterson AFB, Ohio	
13. ABSTRACT This report describes the development, characterization, and human factors evaluation of high visibility electroluminescent displays. Through the development of a greatly improved contrast filter technique and its combination with anti-reflection coatings, it is shown that daylight aircraft cockpit EL displays can be made. The importance of both specular and diffuse reflections are illustrated. A dramatic reduction in the display brightness required for the threshold of rapid readability has been achieved. Improving display visibility by use of high contrast rather than high brightness means that electrical power dissipation for the display can be reduced, and useful display life increased. () ← Distribution of this abstract is unlimited.		

DD FORM 1473
1 JAN 64

UNCLASSIFIED

Security Classification

UNCLASSIFIED

Security Classification

14. KEY WORDS	LINK A		LINK B		LINK C	
	ROLE	WT	ROLE	WT	ROLE	WT
Display Systems Electroluminescent Elements High Contrast Techniques Aircraft Displays Human Factors Display Visibility						

INSTRUCTIONS

1. **ORIGINATING ACTIVITY:** Enter the name and address of the contractor, subcontractor, grantee, Department of Defense activity or other organization (*corporate author*) issuing the report.
- 2a. **REPORT SECURITY CLASSIFICATION:** Enter the overall security classification of the report. Indicate whether "Restricted Data" is included. Marking is to be in accordance with appropriate security regulations.
- 2b. **GROUP:** Automatic downgrading is specified in DoD Directive 5200.10 and Armed Forces Industrial Manual. Enter the group number. Also, when applicable, show that optional markings have been used for Group 3 and Group 4 as authorized.
3. **REPORT TITLE:** Enter the complete report title in all capital letters. Titles in all cases should be unclassified. If a meaningful title cannot be selected without classification, show title classification in all capitals in parenthesis immediately following the title.
4. **DESCRIPTIVE NOTES:** If appropriate, enter the type of report, e.g., interim, progress, summary, annual, or final. Give the inclusive dates when a specific reporting period is covered.
5. **AUTHOR(S):** Enter the name(s) of author(s) as shown on or in the report. Enter last name, first name, middle initial. If military, show rank and branch of service. The name of the principal author is an absolute minimum requirement.
6. **REPORT DATE:** Enter the date of the report as day, month, year; or month, year. If more than one date appears on the report, use date of publication.
- 7a. **TOTAL NUMBER OF PAGES:** The total page count should follow normal pagination procedures, i.e., enter the number of pages containing information.
- 7b. **NUMBER OF REFERENCES:** Enter the total number of references cited in the report.
- 8a. **CONTRACT OR GRANT NUMBER:** If appropriate, enter the applicable number of the contract or grant under which the report was written.
- 8b, 8c, & 8d. **PROJECT NUMBER:** Enter the appropriate military department identification, such as project number, subproject number, system numbers, task number, etc.
- 9a. **ORIGINATOR'S REPORT NUMBER(S):** Enter the official report number by which the document will be identified and controlled by the originating activity. This number must be unique to this report.
- 9b. **OTHER REPORT NUMBER(S):** If the report has been assigned any other report numbers (*either by the originator or by the sponsor*), also enter this number(s).

10. **AVAILABILITY/LIMITATION NOTICES:** Enter any limitations on further dissemination of the report, other than those imposed by security classification, using standard statements such as:

- (1) "Qualified requesters may obtain copies of this report from DDC."
- (2) "Foreign announcement and dissemination of this report by DDC is not authorized."
- (3) "U. S. Government agencies may obtain copies of this report directly from DDC. Other qualified DDC users shall request through _____."
- (4) "U. S. military agencies may obtain copies of this report directly from DDC. Other qualified users shall request through _____."
- (5) "All distribution of this report is controlled. Qualified DDC users shall request through _____."

If the report has been furnished to the Office of Technical Services, Department of Commerce, for sale to the public, indicate this fact and enter the price, if known.

11. **SUPPLEMENTARY NOTES:** Use for additional explanatory notes.

12. **SPONSORING MILITARY ACTIVITY:** Enter the name of the departmental project office or laboratory sponsoring (*paying for*) the research and development. Include address.

13. **ABSTRACT:** Enter an abstract giving a brief and factual summary of the document indicative of the report, even though it may also appear elsewhere in the body of the technical report. If additional space is required, a continuation sheet shall be attached.

It is highly desirable that the abstract of classified reports be unclassified. Each paragraph of the abstract shall end with an indication of the military security classification of the information in the paragraph, represented as (TS), (S), (C), or (U).

There is no limitation on the length of the abstract. However, the suggested length is from 150 to 225 words.

14. **KEY WORDS:** Key words are technically meaningful terms or short phrases that characterize a report and may be used as index entries for cataloging the report. Key words must be selected so that no security classification is required. Identifiers, such as equipment model designation, trade name, military project code name, geographic location, may be used as key words but will be followed by an indication of technical context. The assignment of links, rules, and weights is optional.

UNCLASSIFIED

Security Classification